Gamma-Ray Absorption Coefficients*

CHARLOTTE MEAKER DAVISSON† AND ROBLEY D. EVANS

Massachusetts Institute of Technology, Cambridge, Massachusetts

A survey is given of the absorption of radiation in the energy range from 0.1 Mev to 6 Mev. Results of the theories of Compton effect, photoelectric effect, and pair production are given in the form of equations, tables, and curves. Necessary considerations in studying absorption coefficients are discussed and results of various workers are compared with theory. It is concluded that in this energy range the present theories give values of absorption coefficients which are in good agreement with those obtained experimentally.

INTRODUCTION

WITH the increasing use of radioactive materials, it is becoming important to know with some accuracy how the interaction of γ-rays with matter varies with γ-ray energy. Theories for the different types of γ-ray interaction with matter have been developed. It is the purpose of this paper to compile, for the energy range from 0.1 Mev to 6 Mev, the results of the existing theories of γ-ray absorption and the values they predict, to discuss the measurement of γ-ray absorption coefficients, and to compare the results of various experimental studies of γ-ray absorption with the theories.

In our calculations we have used for the fundamental constants the values given by Birge.[1] These, as well as some derived quantities which we have used, are given in Table I. Although in many of our following tables four figures are given, not more than three can be considered significant.

GENERAL THEORY

The basis of all measurements on the absorption of x-rays or γ-rays is the fact that the intensity of radiation decreases as it passes through material in such a way that for a small thickness Δx, the change in intensity ΔI is proportional to the thickness and to the incident intensity I. That is,

$$\Delta I = -\mu I \Delta x, \tag{1}$$

where μ is the proportionality constant and is known as the absorption coefficient or the cross section. If the radiation is homogeneous, μ is constant, and the integration of this equation yields

$$I/I_0 = e^{-\mu x}. \tag{2}$$

This gives the intensity of radiation I after a beam of initial intensity I_0 has traversed the thickness x of a particular material. It may be noted that since $I = h\nu B$ where B is the number of photons crossing unit area in unit time, and $h\nu$ is the energy per photon, we may also write

$$B/B_0 = e^{-\mu x}. \tag{3}$$

The thickness x may be expressed variously as cm, g/cm^2, atoms/cm^2, or electrons/cm^2. Since the product μx must be dimensionless, μ is correspondingly expressed as cm^{-1}, cm^2/g, cm^2/atom, or cm^2/electron. To indicate which unit is being used we shall write ${}_e\mu$ for the value in cm^2/electron, ${}_a\mu$ for cm^2/atom, μ/ρ for cm^2/g, and μ for cm^{-1}. Expressing the last three in terms of cm^2/electron, i.e., ${}_e\mu$, we find that

$${}_a\mu = Z\,{}_e\mu, \tag{4}$$

$$\mu/\rho = N(Z/A)\,{}_e\mu, \tag{5}$$

$$\mu = \rho N(Z/A)\,{}_e\mu, \tag{6}$$

where Z is the atomic number, A the atomic weight, N Avogadro's number, and ρ the density in g/cc. Since, except between hydrogen and helium, Z/A changes very slowly as Z increases, and since, as will be seen later, μ in cm^2/electron is about the same for all elements in a certain energy region, μ shows least variation from element to element when expressed in cm^2/electron or cm^2/g.

In the energy range from 0.1 Mev to 6 Mev three types of γ-ray interaction with matter must be considered: (1) the Compton effect, in which a photon is scattered by an electron of the atom, the photon going off in a different direction with decreased energy and the

TABLE I. Numerical values of constants used in calculations.

1. Basic constants
$e = 4.8025\times10^{-10}$ esu
$e/m = 5.2736\times10^{17}$ esu g^{-1}
$c = 2.9978\times10^{10}$ cm sec^{-1}
$h = 6.6242\times10^{-27}$ erg sec
$A = 6.0228\times10^{23}$ mole^{-1}
$m = 9.1064\times10^{-28}$ g
2. Derived quantities
$r_0 = e^2/mc^2 = 2.8182\times10^{-13}$ cm
$mc^2 = 0.51084$ Mev
$\varphi_0 = 8\pi r_0^2/3 = 6.6537\times10^{-25}$ cm^2
$1/\alpha = \text{“137”} = hc/2\pi e^2 = 137.03$
$\bar{\phi} = r_0^2Z^2/\text{“137”} = 5.7958\times10^{-28}Z^2$ cm^2
1 Mev $= 1.6020\times10^{-6}$ ergs

* This paper is taken in part from a thesis submitted by Charlotte Meaker Davisson in partial fulfillment of the requirements for a degree of Doctor of Philosophy in the physics department of the Massachusetts Institute of Technology. Assisted by the joint program of the ONR and AEC.

† Present address: c/o Dr. J. W. Davisson, Crystal Branch, Naval Research Laboratory, Washington 20, D. C.

[1] Raymond T. Birge, Revs. Modern Phys. **13**, 233 (1941).

electron recoiling with the remaining energy; (2) the photoelectric effect in which a photon gives all its energy to a bound electron which uses part of the energy to overcome its binding to the atom and takes the rest as kinetic energy; and (3) pair production, in which a photon in the field of the nucleus produces an electron-positron pair, whose total kinetic energy is equal to the energy of the photon minus the mass energy of the two particles which have been created. This third method of absorption can take place only when the energy of the photon is equal to or greater than the mass energy of the electron-positron pair.

The three processes act independently of each other so we can separate the absorption coefficient into three parts which we shall designate by σ for Compton effect, τ for photoelectric effect, and κ for pair production. Since Eq. (1) holds for each process separately, i.e.,

$$(\Delta I)_{\text{Compton}} = -\sigma I \Delta x, \tag{7a}$$

$$(\Delta I)_{\text{photoel.}} = -\tau I \Delta x, \tag{7b}$$

$$(\Delta I)_{\text{pr. prod.}} = -\kappa I \Delta x, \tag{7c}$$

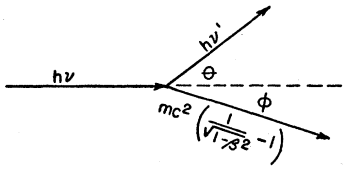

FIG. 1. Compton effect. Angular and energy notations.

we obtain the total intensity change by adding the three, i.e.,

$$\Delta I = -(\sigma+\tau+\kappa) I \Delta x, \tag{7d}$$

so

$$\mu = \sigma+\tau+\kappa. \tag{8}$$

We are interested in seeing how σ, τ, and κ vary with the energy of the photons and the atomic number of the absorber according to the existing theories. We shall therefore consider each one separately.[2]

COMPTON EFFECT

In considering the Compton effect it is assumed that the electrons in the atom may be thought of as free and that the photon collides with an electron and is deflected, the electron recoiling in a different direction. From the conservation of energy and momentum in the process, we obtain, using the relativistic expressions for kinetic energy and mass, and the notation shown in Fig. 1,

$$\begin{aligned} h\nu &= mc^2\left(\frac{1}{(1-\beta^2)^{\frac{1}{2}}}-1\right)+h\nu', \\ \frac{h\nu}{c} &= \frac{mc\beta}{(1-\beta^2)^{\frac{1}{2}}}\cos\varphi+\frac{h\nu'}{c}\cos\theta, \\ 0 &= \frac{mc\beta}{(1-\beta^2)^{\frac{1}{2}}}\sin\varphi-\frac{h\nu'}{c}\sin\theta, \end{aligned} \tag{9}$$

where β is the electron velocity in units of the velocity of light. From these three equations by eliminating any two of the quantities φ, β, θ, ν', we obtain expressions for (1) the energy or wavelength of the scattered photon as a function of θ; (2) the energy of the recoil electron as a function of either θ or φ; and (3) φ as a function of θ. The expressions are

$$h\nu' = \frac{h\nu}{1+\alpha(1-\cos\theta)}, \tag{10}$$

$$E_{\text{electron}} = h\nu\left(1-\frac{1}{1+\alpha(1-\cos\theta)}\right) \tag{11}$$

$$= h\nu\left(\frac{2\alpha}{1+2\alpha+(1+\alpha)^2\tan^2\varphi}\right), \tag{12}$$

$$\cos\theta = 1-\frac{2}{(1+\alpha)^2\tan^2\varphi+1}, \tag{13}‡$$

in which $\alpha = h\nu/mc^2$.

To obtain the fraction of the γ-ray energy scattered in a given direction, Klein and Nishina[3] have carried out a quantum-mechanical treatment of the problem using the Dirac equation for the electron and have obtained the equation

$$I = I_0\frac{e^4}{2m^2c^4r^2}\frac{1+\cos^2\theta}{[1+\alpha(1-\cos\theta)]^3} \times\left\{1+\frac{\alpha^2(1-\cos\theta)^2}{(1+\cos^2\theta)[1+\alpha(1-\cos\theta)]}\right\}, \tag{14}$$

where I_0 is the intensity of the incident beam of γ-rays, I is the intensity of the scattered beam at the angle θ and distance r from the scattering electron of charge e and mass m, and $\alpha = h\nu/mc^2$.

Equation (14) may also be written

$$I = \frac{I_0}{r^2}\frac{h\nu'}{h\nu}k(\theta), \tag{15}$$

where $k(\theta)$ is the cross section for the number of photons scattered per electron and per unit solid angle in the direction θ, and is given by

$$\frac{d_e\sigma(\theta)}{d\Omega} = k(\theta) = \frac{r_0^2}{2}\left\{\frac{1}{[1+\alpha(1-\cos\theta)]^2} \times\left[1+\cos^2\theta+\frac{\alpha^2(1-\cos\theta)^2}{[1+\alpha(1-\cos\theta)]}\right]\right\}. \tag{16}$$

Here $r_0 = e^2/mc^2$ and ${}_e\sigma(\theta)$ is the cross section for the number of photons scattered into the solid angle $d\Omega$ in

[2] See also T. Kahan, J. phys. et radium **10**, 430 (1939).

‡ Also $\cot\varphi = (1+\alpha)\tan(\theta/2)$.

[3] O. Klein and Y. Nishina, Z. Physik **52**, 853 (1929).

the direction θ. For low energies, i.e., for very small values of α, Eq. (16) reduces to

$$k(\theta)=\frac{r_0^2}{2}(1+\cos^2\theta), \tag{17}$$

which is the Thomson equation.[4] The cross section for the amount of energy scattered per electron and per unit solid angle is $(h\nu'/h\nu)k(\theta)$. Calling this $\kappa(\theta)$ and combining Eqs. (16) and (10), we have

$$\frac{d_e\sigma_s(\theta)}{d\Omega}=\kappa(\theta)=\frac{r_0^2}{2}\left\{\frac{1}{[1+\alpha(1-\cos\theta)]^3}\times\left[1+\cos^2\theta+\frac{\alpha^2(1-\cos\theta)^2}{[1+\alpha(1-\cos\theta)]}\right]\right\}, \tag{18}$$

where ${}_e\sigma_s(\theta)$ is the cross section for the energy of the photons scattered into the solid angle $d\Omega$ in the direction θ.

By placing $d\Omega=\sin\theta d\theta d\varphi$ and integrating Eqs. (16), (17), and (18) between different limits for φ and θ, numerous quantities of interest in scattering and absorption measurements can be determined. Some of these are:

1. ${}_e\sigma$ = the Compton total cross section or the cross section for the number of photons scattered.
2. ${}_e\sigma_s$ = Compton scattering coefficient or the cross section for the energy of the photons scattered.
3. ${}_e\sigma_a$ = the Compton absorption coefficient or the cross section for the energy absorbed by the electrons.
4. ${}_e\sigma^{\theta_0}$ = the cross section for the number of photons scattered between 0 and θ_0.
5. ${}_e\sigma_s{}^{\theta_0}$ = the cross section for the energy scattered between 0 and θ_0.
6. ${}_e\sigma_f$ = the cross section for the number of photons scattered forward.
7. ${}_e\sigma_b$ = the cross section for the number of photons scattered backward.
8. ${}_e\sigma_{sf}$ = Compton forward scattering coefficient or the cross section for the energy scattered forward.
9. ${}_e\sigma_{sb}$ = Compton backward scattering coefficient or the cross section for the energy scattered backward.
10. ${}_e\sigma^{\theta_0}/{}_e\sigma$ = the fraction of the scattered photons which are scattered between 0 and θ_0.
11. ${}_e\sigma_s{}^{\theta_0}/{}_e\sigma_s$ = the fraction of the scattered energy which is scattered between 0 and θ_0.

The Compton total cross section ${}_e\sigma$ is obtained by integrating Eq. (16) between 0 and π for θ and 0 and 2π for φ. The result is the well-known equation

$${}_e\sigma=2\pi r_0^2\left\{\frac{1+\alpha}{\alpha^2}\left[\frac{2(1+\alpha)}{1+2\alpha}-\frac{1}{\alpha}\ln(1+2\alpha)\right]+\frac{1}{2\alpha}\ln(1+2\alpha)-\frac{1+3\alpha}{(1+2\alpha)^2}\right\}. \tag{19}$$

[4] J. J. Thompson, *Conduction of Electricity Through Gases* (University Press, Cambridge, England, 1906), second edition, p. 325.

Integrating Eq. (18) between the same limits gives the Compton scattering coefficient, ${}_e\sigma_s$, which is

$${}_e\sigma_s=\pi r_0^2\left[\frac{1}{\alpha^3}\ln(1+2\alpha)+\frac{2(1+\alpha)(2\alpha^2-2\alpha-1)}{\alpha^2(1+2\alpha)^2}+\frac{8\alpha^2}{3(1+2\alpha)^3}\right]. \tag{20}$$

Since ${}_e\sigma$ is the cross section for the number of photons scattered or for the total amount of energy removed from the initial beam and ${}_e\sigma_s$ is the cross section for the amount of energy retained by the scattered photons, ${}_e\sigma_a$, the cross section for the amount of energy absorbed by the electrons, is obtained by subtracting ${}_e\sigma_s$ from ${}_e\sigma$. That is,

$${}_e\sigma={}_e\sigma_s+{}_e\sigma_a. \tag{21}$$

It may be noted that ${}_e\sigma_s$ and ${}_e\sigma_a$ apply only to the partial energy which is removed from the original beam and apply separately only to intensity considerations. For consideration of the number of photons removed from the beam it is necessary to use the total[5] coefficient ${}_e\sigma$. Values of ${}_e\sigma$, ${}_e\sigma_s$, and ${}_e\sigma_a$ calculated from these equations are given in Table II and are plotted in Fig. 2 for energies from 0.01 Mev to 10 Mev.

Values of the differential cross sections of Eqs. (16), (17), and (18)[6] are given in Tables III and IV and are plotted in Figs. 3 and 4. These might be called the differential cross sections per unit solid angle. If Eqs. (16), (17), and (18) are integrated only over φ and from $\varphi=0$ to $\varphi=\pi$, cross sections are obtained which might be called the differential cross sections per unit angle. That is, they are the cross sections for the number of photons and for the energy of the photons scattered between two cones whose half angles differ by unity. Since $k(\theta)$ and $\kappa(\theta)$ are not functions of φ, these cross sections are

$$(1/d\theta)\int_{\varphi=0}^{\varphi=2\pi} d_e\sigma(\theta)=2\pi\sin\theta k(\theta), \tag{22}$$

$$(1/d\theta)\int_{\varphi=0}^{\varphi=2\pi} d_e\sigma_s(\theta)=2\pi\sin\theta\kappa(\theta). \tag{23}$$

Expressing it differently we may say that $2\pi\sin\theta k(\theta)d\theta$ is the cross section for the number of photons scattered between two cones of half-angles θ and $\theta+d\theta$, and similarly for the energy. Values of these differential

[5] For detectors whose sensitivity is a function of photon energy, the effective or measured coefficient will lie between $\sigma_s+\sigma_a$ and σ_a depending on the degree of collimation.

[6] Values for $\kappa(\theta)$ have also been calculated and tabulated by Tarrant [Proc. Cambridge Phil. Soc. 28, 475 (1932)]. For r_0^2 he used the value of 3.9497×10^{-26}, whereas we have used 3.9711×10^{-26}. When correction is made for this, our values agree with his. However, for $\alpha=1$ and greater and angles less than 60° we do not agree with the curves given by W. Heitler [*The Quantum Theory of Radiation* (Oxford University Press, London, 1936), p. 156].

TABLE II. Cross sections for the Compton effect ${}_e\sigma = {}_e\sigma_a + {}_e\sigma_s$ (in units of 10^{-25} cm²/electron).

$\alpha = h\nu/mc^2$	${}_e\sigma$	${}_e\sigma_s$	${}_e\sigma_a$
0.025	6.31	6.31	0.00
0.05	6.07	5.79	0.28
0.075	5.83		
0.1	5.599	5.138	0.461
0.125	5.409		
0.15	5.243		
0.20	4.900	4.217	0.683
0.25	4.636		
1/3	4.273		
0.40	4.032	3.152	0.880
0.50	3.744		
2/3	3.369		
0.80	3.140	2.158	0.982
1.0	2.866	1.879	0.987
4/3	2.529	1.553	0.976
1.635	2.303		
2.0	2.090	1.164	0.926
2.232	1.979		
2.418	1.901		
8/3	1.806		
3.0	1.696	0.8523	0.844
4.0	1.446	0.6745	0.772
5.155	1.246		
5.403	1.211		
6.0	1.136	0.4774	0.659
8.0	0.9465	0.3700	0.5765
10.0	0.8168	0.3023	0.5145
12.0	0.7215		
20.0	0.5019	0.1581	0.3438
30.0	0.3710	0.1071	0.2639
100/3	0.3424		
50.0	0.2498	0.06596	0.1838
70.0	0.1911	0.04719	0.1439
100.0	0.1431	0.03302	0.1101

cross sections [Eqs. (22) and (23)] are plotted in Figs. 5 and 6.

If Eqs. (16), (17), and (18) are integrated over φ from 0 to 2π and over θ from 0 to θ_0, the cross sections ${}_e\sigma^{\theta_0}$ and ${}_e\sigma_s{}^{\theta_0}$ for the number and the energy of the photons scattered between $\theta=0$ and $\theta=\theta_0$ are obtained. If one

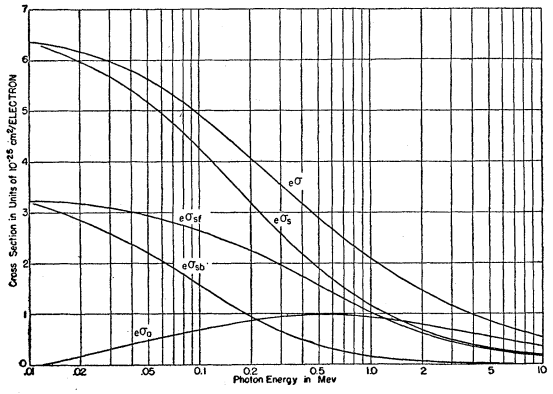

FIG. 2. Compton effect. Cross sections *vs* energy. ${}_e\sigma$ the cross section for the number of photons scattered; ${}_e\sigma_s$ the cross section for the energy of the photons scattered; ${}_e\sigma_a$ the cross section for the energy absorbed by the electrons; ${}_e\sigma_{sf}$ the cross section for the photon energy scattered forward; ${}_e\sigma_{sb}$ the cross section for the photon energy scattered backward.

TABLE III. Compton effect. Differential cross section per unit solid angle for the number of photons scattered at the angle θ [Eq. (16)] (in units of 10^{-26} cm²/electron).

θ (degrees)	$\alpha=0$	$\alpha=0.1$	$\alpha=0.4$	$\alpha=1.0$	$\alpha=4.0$	$\alpha=10$
0	7.94	7.94	7.94	7.94	7.94	7.94
2						7.84
5					7.68	7.35
7						6.85
10	7.82	7.80	7.73	7.59	6.96	5.96
12						5.34
14					6.20	4.74
16						4.19
18						3.70
20	7.48	7.39	7.13	6.66	4.97	3.26
25					4.04	2.41
30	6.95	6.77	6.27	5.45	3.26	1.82
40	6.30	6.02	5.29	4.25	2.16	1.15
50	5.61	5.24	4.35	3.25	1.52	
55	5.28					
60	4.96	4.51	3.54	2.50	1.14	0.597
70	4.44	3.92	2.92	1.99	0.910	
80	4.09	3.51	2.50	1.67	0.764	
90	3.97	3.31	2.26	1.49	0.667	0.331
100	4.09	3.32	2.17	1.40		
110	4.44	3.50	2.19	1.37	0.552	
120	4.96	3.81	2.29	1.37		0.238
130	5.61	4.22	2.42		0.493	
140	6.30	4.63	2.56	1.41		
150	6.95	5.02	2.69		0.462	0.190
160	7.48	5.33	2.80	1.45		
170	7.82	5.54	2.86			
180	7.94	5.61	2.89	1.47	0.447	0.190

uses the Thomson equation (17), this becomes

$$ {}_e\sigma^{\theta_0} = (\pi r_0^2/3)(4-3\cos\theta_0-\cos^3\theta_0). \qquad (24)$$

TABLE IV. Compton effect. Differential cross section per unit solid angle for the energy of photons scattered at the angle θ [Eq. (18)] (in units of 10^{-26} cm²/electron).

θ (degrees)	$\alpha=0$	$\alpha=0.1$	$\alpha=0.4$	$\alpha=1.0$	$\alpha=4.0$	$\alpha=10$
0	7.94	7.94	7.94	7.94	7.94	7.94
2						7.80
5					7.51	7.08
7						6.37
10	7.82	7.79	7.68	7.48	6.57	5.17
12						4.38
14					5.54	3.66
16						3.02
18						2.48
20	7.48	7.34	6.97	6.28	4.01	2.03
25					2.94	1.24
30	6.95	6.68	5.95	4.81	2.13	0.780
40	6.30	5.88	4.84	3.45	1.12	0.344
50	5.61	5.06	3.81	2.40	0.625	
55	5.28					
60	4.96	4.30	2.95	1.67	0.380	0.0996
70	4.44	3.68	2.31	1.20	0.251	
80	4.09	3.24	1.88	0.915	0.177	
90	3.97	3.01	1.61	0.744	0.133	0.0301
100	4.09	2.97	1.48	0.643		
110	4.44	3.08	1.43	0.583	0.0867	
120	4.96	3.32	1.43	0.547		0.0149
130	5.61	3.61	1.46		0.0651	
140	6.30	3.93	1.50	0.510		
150	6.95	4.23	1.54		0.0546	0.00965
160	7.48	4.47	1.58	0.494		
170	7.82	4.62	1.60			
180	7.94	4.67	1.60	0.490	0.0496	0.00903

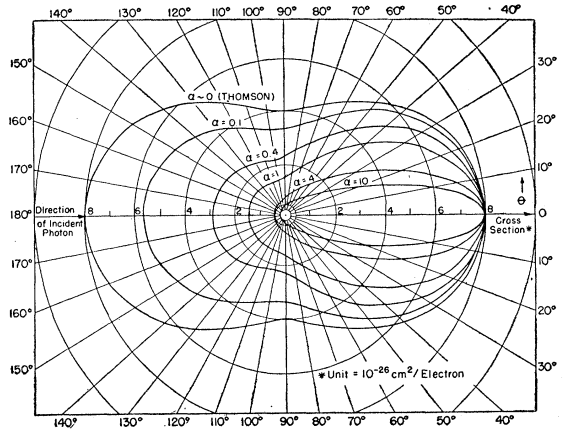

FIG. 3. Compton effect. Differential cross section per unit solid angle for the number of photons scattered at the angle θ [Eq. (16)].

Integrating Eq. (16) we obtain

$$ {}_e\sigma^{\theta_0} = \pi r_0^2 \Big\{ \frac{1}{2\alpha^2(1+\alpha-\alpha\cos\theta_0)^2} [4+10\alpha+8\alpha^2+\alpha^3 - (4+16\alpha+16\alpha^2+2\alpha^3)\cos\theta_0 + (6\alpha+10\alpha^2+\alpha^3)\cos^2\theta_0 - 2\alpha^2\cos^3\theta_0] + \Big(\frac{\alpha^2-2\alpha-2}{\alpha^3}\Big)\ln(1+\alpha-\alpha\cos\theta_0)\Big\} \quad (25) $$

and integrating Eq. (18) yields

$$ {}_e\sigma_s^{\theta_0} = \pi r_0^2 \{ \alpha^{-3}\ln(1+\alpha-\alpha\cos\theta_0) - [6\alpha^2(1+\alpha-\alpha\cos\theta_0)^3]^{-1} \times [6+15\alpha+3\alpha^2-12\alpha^3-8\alpha^4 - (6+30\alpha+27\alpha^2-18\alpha^3-24\alpha^4)\cos\theta_0 + (15\alpha+33\alpha^2-24\alpha^4)\cos^2\theta_0 - (9\alpha^2+6\alpha^3-8\alpha^4)\cos^3\theta_0] \}. \quad (26) $$

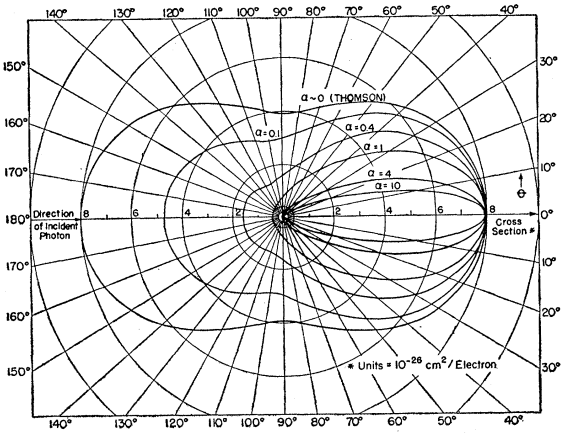

FIG. 4. Compton effect. Differential cross section per unit solid angle for the photon energy scattered at the angle θ [Eq. (18)].

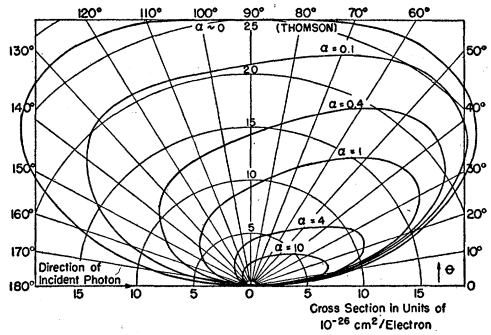

FIG. 5. Compton effect. Differential cross section per unit angle for the number of photons scattered in the direction θ [Eq. (22)].

[For $\theta_0=\pi$ these become Eqs. (19) and (20).] For small angles the following approximations to Eqs. (25) and (26) may be used:

($<15°$ to $20°$)

$$ {}_e\sigma^{\theta_0} = \pi r_0^2 \{ [1+\alpha-\alpha\cos\theta_0]^{-2} \times [(2\alpha+2)(1-\cos\theta_0)^2+\cos\theta_0\sin^2\theta_0] \}, \quad (27) $$

$$ {}_e\sigma_s^{\theta_0} = \pi r_0^2 \{ [3(1+\alpha-\alpha\cos\theta_0)^3]^{-1} \times [4+6\alpha+4\alpha^2-(3+9\alpha+12\alpha^2)\cos\theta_0 + 12\alpha^2\cos^2\theta_0-(1-3\alpha+4\alpha^2)\cos^3\theta_0] \}, \quad (28) $$

($<10°$)

$$ {}_e\sigma^{\theta_0} = \pi r_0^2\theta_0^2[1-(\theta_0^2/6)(3\alpha+2)], \quad (29) $$

$$ {}_e\sigma_s^{\theta_0} = \pi r_0^2\theta_0^2[1-(\theta_0^2/12)(9\alpha+4)], \quad (30)\S $$

($<5°$)

$$ {}_e\sigma^{\theta_0} = {}_e\sigma_s^{\theta_0} = \pi r_0^2\theta_0^2. \quad (31) $$

Values for ${}_e\sigma^{\theta_0}$ and ${}_e\sigma_s^{\theta_0}$ are given in Tables V and VI. For small angles they are plotted in Fig. 7.

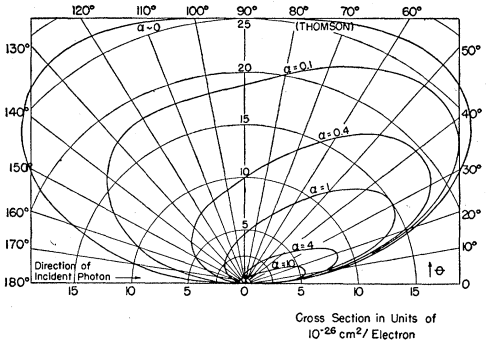

FIG. 6. Compton effect. Differential cross section per unit angle for the photon energy scattered in the direction θ [Eq. (23)].

§ This does not agree with the equation given by Tarrant [see footnote 6]. He gives

$$ {}_e\sigma_s^{\theta_0} = \pi r_0^2\theta_0^2\{1+(\theta_0^2/4)[(11/2)\alpha-1]\}. $$

We can find no mistake in our algebra. Also, values calculated from his equation deviate from the correct value more than those calculated from the still poorer approximation of Eq. (31).

TABLE V. Compton effect. Cross section for the number of photons scattered between 0 and θ_0 [Eqs. (25), (27), (29), and (31)] (in units of 10^{-27} cm²/electron).

θ_0 (degrees)	$\alpha=0$	$\alpha=0.1$	$\alpha=0.2$	$\alpha=0.4$	$\alpha=0.6$	$\alpha=0.8$	$\alpha=1$	$\alpha=2$	$\alpha=4$	$\alpha=6$	$\alpha=8$	$\alpha=10$
0.5		0.0190	0.0190	0.0190	0.0190	0.0190	0.0190	0.0190	0.0190	0.0190	0.0190	0.0190
1.0		0.0760	0.0760	0.0760	0.0760	0.0760	0.0760	0.0760	0.0759	0.0759	0.0759	0.0759
1.5		0.1710	0.1710	0.1709	0.1709	0.1709	0.1709	0.1709	0.1707	0.1706	0.1705	0.1704
2.0		0.3039	0.3039	0.3038	0.3038	0.3038	0.3037	0.3035	0.3032	0.3028	0.3024	0.3021
2.5							0.48					
3							0.68					
4		1.214	1.214	1.213	1.212	1.212	1.211	1.208	1.202	1.197	1.191	1.185
5				1.892			1.888		1.866			1.826
6		2.725	2.723	2.720	2.717	2.715	2.711	2.697	2.668	2.640	2.612	2.597
7				3.695			3.678		3.599			3.450
10	7.5	7.512	7.502	7.480	7.457	7.435	7.413	7.304	7.097	6.900	6.714	6.55
15		16.75	16.61	16.50	16.39	16.29	16.18	15.68	14.75	13.92	13.19	12.67
20	29.2	29.07	28.90	28.57	28.25	27.93	27.63	26.15	23.69	21.74	19.91	18.9
30	62.6	61.63		59.96			55.76	50.08	42.4			30.1
40	104.2			95.46			85.7	73.8	58.9			39.1
50	150	146		133			114	94.8	72.9			46.4
60	198						140					
70	244	230		199			162	128	94.7			57.9
80	289											
90	333	307		254			198	153	111			66.3
100	376											
110	421	377		301			229	174	124			72.6
120	468						242					
150	604	514										
180	665											

The forward scattering coefficients ${}_e\sigma_f$ and ${}_e\sigma_{sf}$ are obtained by integrating Eqs. (16), (17), and (18) between $\varphi=0$ and 2π and $\theta=0$ and $\pi/2$ [or placing $\theta_0=\pi/2$ in Eqs. (24), (25), and (26)]. Doing this we obtain from the Thomson equation

$$ {}_e\sigma_f=4\pi r_0^2/3, \tag{32}$$

and from the others

$$ {}_e\sigma_f=\pi r_0^2\{[4+10\alpha+8\alpha^2+\alpha^3]/[2\alpha^2(1+\alpha)]\}, \tag{33}$$

$$ {}_e\sigma_{sf}=\pi r_0^2\{\alpha^{-3}\ln(1+\alpha) -[6+15\alpha+3\alpha^2-12\alpha^3-8\alpha^4]/[6\alpha^2(1+\alpha)^3]\}. \tag{34}$$

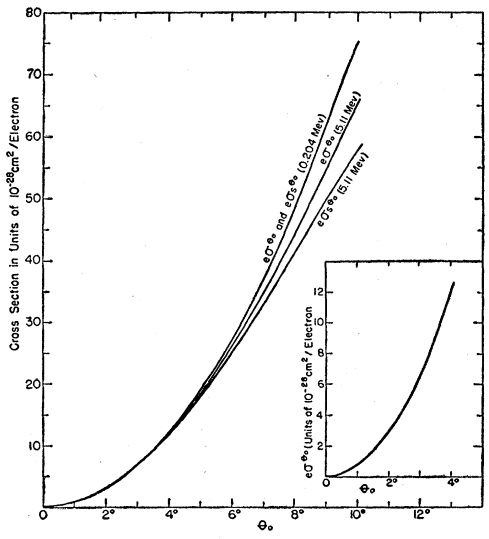

FIG. 7. Compton effect. Cross section at small angles for the number of photons (${}_e\sigma^{\theta_0}$) and for the energy of the photons (${}_e\sigma_s{}^{\theta_0}$) scattered between 0 and θ_0 [Eqs. (29), (30), (31)].

The backward scattering coefficients are obtained by subtraction, since

$$ {}_e\sigma={}_e\sigma_f+{}_e\sigma_b \tag{35}$$

and

$$ {}_e\sigma_s={}_e\sigma_{sf}+{}_e\sigma_{sb}. \tag{36}$$

Numerical values of the forward scattering coefficients are given in Tables V and VI under the values for $\theta_0=90°$. The coefficients for the energy scattered forward and backward, ${}_e\sigma_{sf}$ and ${}_e\sigma_{sb}$, are plotted in Fig. 2.

Values for the fraction of the scattered photons which are scattered between 0 and θ_0, i.e., ${}_e\sigma^{\theta_0}/{}_e\sigma$ and the fraction of the scattered energy which is scattered between 0 and θ_0, i.e., ${}_e\sigma_s{}^{\theta_0}/{}_e\sigma_s$ are plotted in Figs. 8 and 9.

For a discussion of Compton electrons see the appendix.

TABLE VI. Compton effect. Cross section for the energy of photons scattered between 0 and θ_0 [Eqs. (26), (28), (30), and (31)] (in units of 10^{-27} cm²/electron).

θ_0 (deg)	$\alpha=0$	$\alpha=0.1$	$\alpha=0.4$	$\alpha=1$	$\alpha=2$	$\alpha=4$	$\alpha=10$
1			0.0760	0.0760	0.0760	0.0759	0.0758
2			0.3038	0.3036	0.3033	0.3028	0.3011
3			0.682	0.679			
5			1.891	1.884	1.874	1.852	1.787
7			3.690	3.664	3.622	3.539	3.290
10	7.5	7.507	7.46	7.36	7.18	6.83	5.79
15			16.38	15.92	15.2	13.8	11.4
20	29.2	28.95	28.2	26.78	24.75	21.46	13.9
25			42.3	39.2			
30	62.6	61.63	58.00	52.28	44.88	34.99	21
40	104.2		91.80	77.9	62.31	44.67	24
50	150	142.7	122.8	100.2	75.6	51.13	26
70	244	225.1	181.0	132.1	92.4	58.6	28.3
90	333	295	221.9	152.2	102.0	62.5	29.2
110	421	359	254.1	166.1	108.2	64.8	
130	515	427					
150	604	474					
180	665						

PHOTOELECTRIC EFFECT

Theoretical analyses of the photoelectric process have been made, but exact solutions of the equations are both difficult and tedious, since the Dirac relativistic equation for a bound electron must be used. In the energy region of 0.35 Mev to 2 Mev the exact solution has been obtained by Hulme, McDougall, Buckingham, and Fowler.[7] At other energies approximations can be made which simplify the solution somewhat. The theoretical results can therefore be divided into three energy regions: (1) energies greater than 2 Mev, (2) energies from 0.35 Mev to 2 Mev, and (3) energies below 0.35 Mev.

1. Energies Greater than 2 Mev

Hall[8] has expanded the wave function in powers of the photon wavelength (reciprocal of the photon energy). For energies large compared with mc^2 only the first terms of the expansion need be considered. Thus, using

TABLE VII. Photoelectric effect. Absorption coefficients calculated from Hall's formula [Eq. (37)].

	$n=0$ $h\nu\to\infty$	$n=0.1$ $h\nu=5.108$ Mev		$n=0.194$ $h\nu=2.62$ Mev	
Z	${}_a\tau/Z^5n$ $\times10^{32}$	${}_a\tau/Z^5n$ $\times10^{32}$	${}_a\tau$	${}_a\tau/Z^5n$ $\times10^{32}$	${}_a\tau$
0	0.354	0.436	...	0.524	...
13	0.279	0.343	1.27×10^{-28}	0.412	2.96×10^{-28}
26	0.236	0.289	3.43×10^{-27}	0.347	7.99×10^{-27}
38	0.210	0.255	2.02×10^{-26}	0.302	4.65×10^{-26}
50	0.192	0.230	7.20×10^{-26}	0.270	1.65×10^{-25}
65	0.175	0.206	2.39×10^{-25}	0.237	5.34×10^{-25}
82	0.160	0.182	6.75×10^{-25}	0.205	1.47×10^{-24}

only terms of the order $1/\epsilon$, Hall obtains the equation[9]

$$\frac{{}_a\tau_K}{Z^5n}=\frac{(3/2)\varphi_0(1/137)^4}{\eta^{2\eta^2}e^{\eta(\pi-2\eta)}}\left\{k_0'^3\epsilon n^4\left[\frac{4}{3\epsilon}+\frac{\epsilon-2}{\epsilon+1}\times\left(1+\frac{1}{2\epsilon k_0'}\ln\frac{\epsilon-k_0'}{\epsilon+k_0'}\right)\right]\right\},\quad(37)$$

where ${}_a\tau_K$ is the photoelectric absorption coefficient due to absorption by the two electrons in the K shell only, in cm^2/atom, Z is the atomic number, n is $mc^2/h\nu=(mc/h)\lambda$, 137 is $hc/2\pi e^2$, φ_0 is $8\pi r_0^2/3$ or the Thomson cross section, η is $Z/137$, ϵ is $(1/n)+(1-\eta^2)$ or the total energy of the photoelectron in units of mc^2, and k_0' is $(\epsilon^2-1)^{\frac{1}{2}}$ or $c\times$the momentum of the photoelectron in units of mc^2. At 1.13 Mev the values given by this equation agree with the more rigorous calculations of Hulme *et al.*[7] within 8 percent. At higher energies the agreement should be even better.

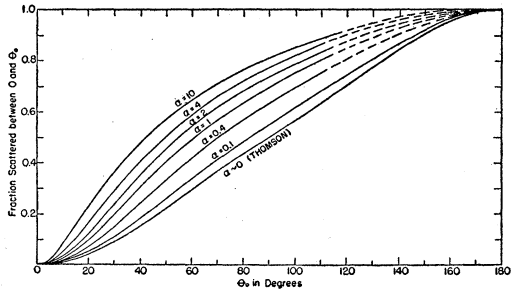

FIG. 8. Compton effect. Fraction of scattered photons which are scattered between 0 and θ_0.

Values calculated from this equation are given in Table VII. The values in the table are the atomic absorption coefficient ${}_a\tau$ obtained from ${}_a\tau_K$ by multiplying by 5/4. This is done to include the effect of the outer shells, since it has been shown both theoretically[10,11] and experimentally[12,13] that throughout the energy range we are considering about $\frac{4}{5}$ of the photoelectric absorption is due to the K shell.

2. Energies from 0.35 Mev to 2 Mev

In this energy region Hulme, McDougall, Buckingham, and Fowler[7] have carried out a rigorous numerical calculation assuming only that exchange interactions between atomic electrons may be neglected, each K electron being treated separately and that the system consists of a fixed nucleus and one K electron, so that the results are doubled to give the total absorption of the K shell. Since the integrations involved yield the sum of a number of hypergeometric functions, no simple formula for the cross section as a function of energy and atomic number can be given. Hulme *et al.* calculated the absorption coefficients for two energies, 0.354 Mev and

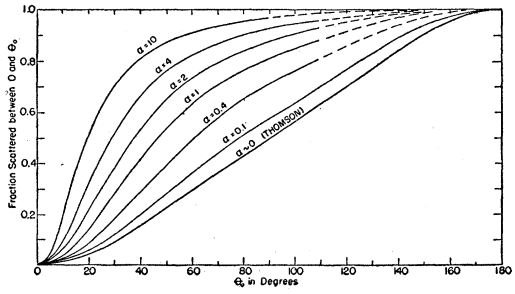

FIG. 9. Compton effect. Fraction of scattered photon energy which is scattered between 0 and θ_0.

[7] Hulme, McDougall, Buckingham, and Fowler, Proc. Roy. Soc. (London) **149A**, 131 (1935).

[8] Harvey Hall, Phys. Rev. **45**, 620 (1934); Revs. Modern Phys. **8**, 358 (1936); Phys. Rev. **84**, 167 (1951).

[9] In his article Hall used α instead of η, $mc^2/h\nu$ and $1/\kappa'$ instead of n, α_0 instead of 1/137, and $4\pi a_0^2\alpha_0^4$ instead of $(3/2)\varphi_0$.

[10] M. Stobbe, Ann. Physik **7**, 661 (1930).

[11] Harvey Hall and William Rarita, Phys. Rev. **46**, 143 (1934).

[12] Rutherford, Chadwick, and Ellis, *Radiations from Radioactive Substances* (Cambridge University Press, London, 1930), p. 464.

[13] Z. S. Davidson and G. D. Latyshev, J. Phys. (U.S.S.R.) **6**, 15 (1942).

TABLE VIII. Photoelectric effect. Absorption coefficients obtained from Hulme,[a] values calculated from Sauter's Eq. (38),[b] and nonrelativistic values from Eq. (39).

			$(_a\tau/Z^5n)\times10^{32}$				
			Values from Sauter				
n	Mev	Values from Hulme	$Z=0$	$Z=13$	$Z=26$	$Z=38$	Non-relativistic values
0.25	2.043	0.489	0.5848	0.6024			0.0414
0.452	1.13		0.8760				
0.50	1.022	0.935		0.9595			0.2342
1.00	0.5108	2.48	2.451	2.435	2.373	2.277	1.325
1.443	0.354		4.825				
2.00	0.2554		9.320	9.433		8.477	7.496
2.50	0.2043	16.8	15.66				13.09
3.00	0.1702		23.78	23.42	22.14	20.15	20.66
4.00	0.1277	50.1	46.80	45.88			42.40
5.00	0.1022		79.90	76.72	71.28	60.95	74.07

[a] H. R. Hulme, Proc. Roy. Soc. (London) **133A**, 381 (1931).
[b] The values used for E_B in Sauter's equation were taken from Compton and Allison, reference 54, p. 792, after correcting to standard wavelengths.

1.13 Mev, and three atomic numbers, $Z=26$, 50, and 84. Using these six values and also values for $Z=0$ taken from an equation obtained by Sauter[14] [Eq. (38)] which is correct at these energies for $Z=0$, they obtain curves for $_a\tau_K/Z^5$ *vs* Z. Using these curves and also the values given by Hall's equation for $n=0$ and $n=0.194$, they obtain values for $_a\tau/Z^5n$ for different values of Z and plot the results as curves. From these curves values of $_a\tau$ may be obtained for any Z and any energy larger than 0.35 Mev. The authors state that the results obtained from their figures should be accurate within 4 percent.

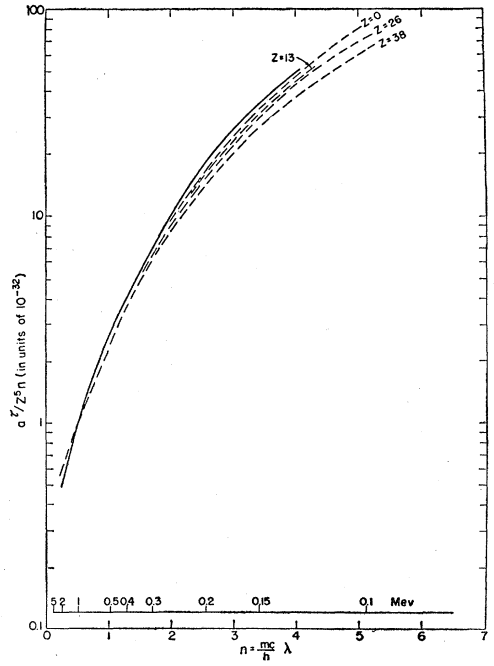

FIG. 10. Photoelectric effect. Comparison of Hulme's values (solid curve) with values from Sauter's equation (dashed curves) [Table VIII and Eq. (38)].

[14] F. Sauter, Ann. Physik **11**, 454 (1931).

3. Energies from 0.1 Mev to 0.35 Mev

In this energy region there are no theoretical results which join smoothly to the results of Hulme *et al.* at 0.35 Mev ($n=1.5$) for all Z. Relativistic calculations have been made by Sauter[14] and Hulme[15] which are valid for $Z/137\ll1$, while nonrelativistic calculations have been made by Fischer,[16] Sauter,[17] and Heitler.[18]

(a) *Relativistic Calculations*

Sauter's result is in the form of an equation which can be written

$$_a\tau_K=\tfrac{3}{2}\varphi_0\frac{Z^5}{(137)^4}n^5(\gamma^2-1)^{\frac{3}{2}}\left[\frac{4}{3}+\frac{\gamma(\gamma-2)}{\gamma+1}\times\left(1-\frac{1}{2\gamma(\gamma^2-1)^{\frac{1}{2}}}\ln\frac{\gamma+(\gamma^2-1)^{\frac{1}{2}}}{\gamma-(\gamma^2-1)^{\frac{1}{2}}}\right)\right], \quad (38)$$

TABLE IX. Photoelectric effect. Correction factor for absorption edge [Eq. (40)].[a]

		$f(\xi)$					
n	Mev	$Z=13$	$Z=26$	$Z=38$	$Z=50$	$Z=65$	$Z=82$
1	0.5108	0.8452	0.7066	0.6024	0.5154	0.4256	0.3435
2	0.2554	0.7907	0.6194	0.5003	0.4121	0.3178	0.2415
3	0.1702	0.7521	0.5617	0.4374	0.3444	0.2583	0.1882
4	0.1277	0.7215	0.5192	0.3922	0.3012	0.2187	0.1540
5	0.1022	0.6962	0.4851	0.3574	0.2680	0.1900	0.1298
8	0.06385	0.6371	0.4116	0.2862	0.2039	0.1351	···
10	0.05108	0.6054	0.3771	0.2525	0.1745	···	···

[a] See reference b of Table VIII.

where

$$\gamma=\frac{1}{(1-\beta^2)^{\frac{1}{2}}}=\frac{h\nu-E_B+mc^2}{mc^2}=\frac{\text{total electron energy}}{\text{electron mass energy}}.$$

E_B is the binding energy of a K electron, and the other symbols are the same as those used in Eq. (37). Since E_B differs from element to element, $_a\tau_K/Z^5n$ obtained from this equation is different for different elements. Hulme's calculations are numerical for different energies and show only a Z^5 dependence of $_a\tau_K$ on Z. Hulme's values, as well as values calculated from Sauter's Eq. (38) for $Z=0$, 13, 26, and 38 are given in Table VIII and are plotted in Fig. 10.

(b) *Nonrelativistic Calculations*

Neglecting the binding energy of the K electrons, Heitler[18] obtains the equation

$$_a\tau_K=\varphi_0Z^5(1/137)^4 4\sqrt{2}(n)^{7/2}, \quad (39)$$

the symbols being the same as in Eq. (37). Values of

[15] H. R. Hulme, Proc. Roy. Soc. (London) **133A**, 381 (1931).
[16] J. Fischer, Ann. Physik **8**, 821 (1931).
[17] F. Sauter, Ann. Physik **9**, 217 (1931).
[18] W. Heitler, *The Quantum Theory of Radiation*, (Oxford University Press, New York, 1936), p. 123.

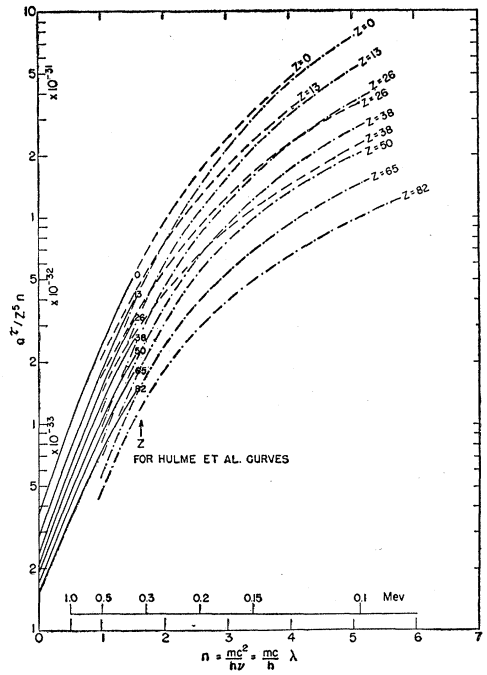

FIG. 11. Photoelectric effect. Comparison of cross sections calculated from different equations. *Solid curves:* from Hulme *et al.* values. *Dashed curves:* from Sauter's Eq. (38) combined with Eq. (40). *Dot and dashed curves:* nonrelativistic Eq. (39) combined with Eq. (40).

$_a\tau/Z^5n$ calculated from this equation are given in the last column of Table VIII. As the energy of the photons approaches that of the K absorption edge, the binding energy of the K electrons cannot be neglected, and $_a\tau_K$ must be multiplied by the correction factor $f(\xi)$ given by Stobbe.[10] This is

$$f(\xi)=2\pi\left(\frac{E_B}{h\nu}\right)^{\frac{1}{2}}\frac{e^{-4\xi \operatorname{arc\,ctg}\xi}}{1-e^{-2\pi\xi}}, \qquad (40)$$

where $\xi=[E_B/(h\nu-E_B)]^{\frac{1}{2}}$. Values of this correction factor for different energies and atomic numbers are given in Table IX. The nonrelativistic equation obtained by Fischer[16] is exactly the same as the product of Eqs. (39) and (40) if terms in $h\nu/2\,mc^2$, $(h\nu/2\,mc^2)^{\frac{1}{2}}$, and β^2 appearing in Fischer's equation are neglected.

(c) *Choosing the Best Values*

Applying the correction factor $f(\xi)$ to the values given in Table VIII for Sauter's results and for the nonrelativistic results, one obtains the curves shown in Fig. 11. The Sauter curves join reasonably well with those of Hulme *et al.* at $n=1.5$ (0.35 Mev), but the nonrelativistic values for large Z fall far below those of Hulme *et al.* To get better values for large Z, a smooth curve has been drawn between the values of Hulme *et al.* and the nonrelativistic values at energies close to the K absorption edges, where nonrelativistic values should give correct results. These interpolated curves are shown in Fig. 12.

4. Summary of Theoretical Photoelectric Coefficients

For ease in obtaining curves of the photoelectric absorption coefficients as a function of energy for a given element, values of $_a\tau/Z^5n$ as a function of Z have been plotted for different energies in Figs. 13 to 17. The points shown on the various curves are given in Table X and were obtained as follows:

(a) For $n=0$, 0.1, and 0.194 the values from Hall's[8] equation (Table VII) were used.

(b) For $n=0.125$ to 1.5 the points shown are those taken from the curves given by Hulme, McDougall, Buckingham, and Fowler.[7] A pair of dividers and scale were used.

(c) For $n=2$ to 5 the points for $Z=13$, 26, and 38 represent values from Sauter's Eq. (38) combined with Eq. (40), while the points for $Z=50$, 65, and 82 were obtained from Fig. 12. The discrepancies from the smooth curve drawn through the points, especially at $Z=38$ indicate the error involved in using Sauter's equation at a value of Z of this size.

5. Comparison with Empirical Formulas

Victoreen[19] has developed an empirical equation for photoelectric absorption coefficients in the energy range

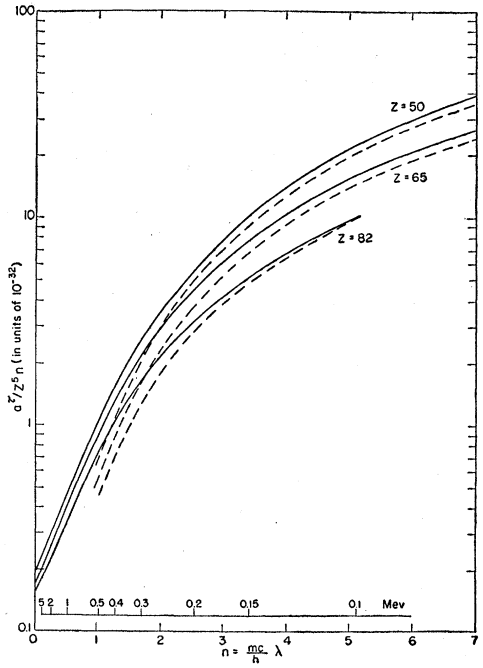

FIG. 12. Photoelectric effect. Interpolation curves for large Z. *Dashed curves:* nonrelativistic Eq. (39) combined with Eq. (40). *Solid curves:* Hulme *et al.* values up to $n=1.5$ joined to nonrelativistic values at $n=10$ for $Z=50$, $n=8$ for $Z=65$, and $n=5$ for $Z=82$.

[19] John A. Victoreen, J. Appl. Phys. **14**, 95 (1943); **19**, 855 (1948).

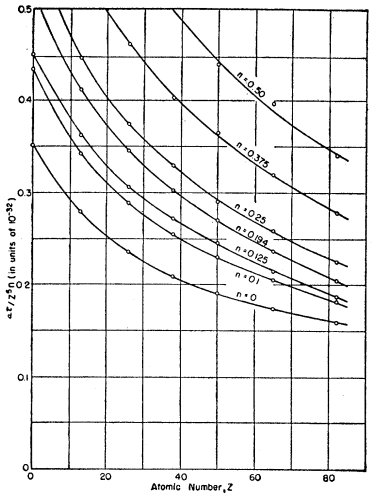

FIG. 13.

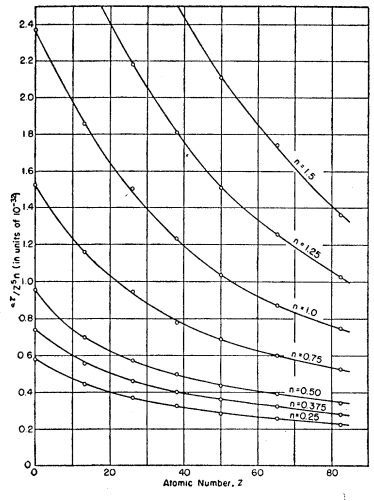

FIG. 14.

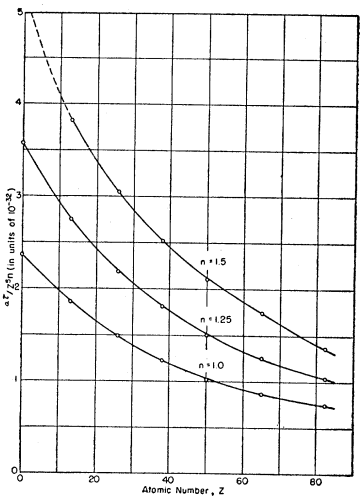

FIG. 15.

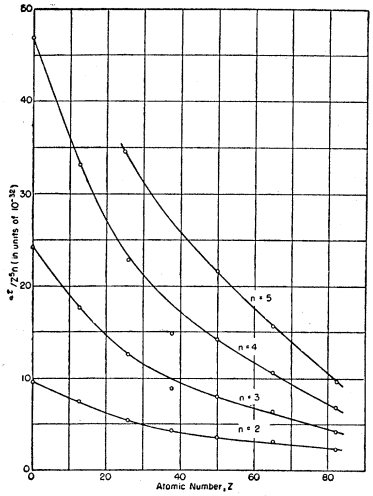

FIG. 16.

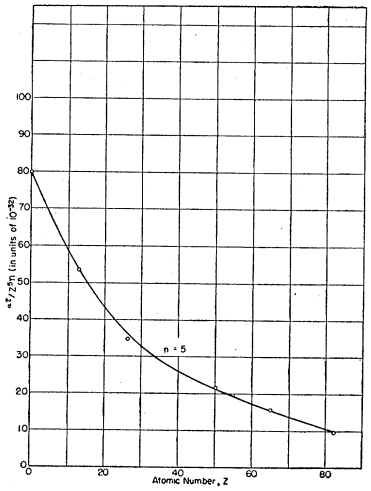

FIG. 17.

FIGS. 13 to 17. Photoelectric effect. Summary of theoretical photoelectric cross sections *vs* atomic number for different energies ($n=mc^2/h\nu$).

from about 1 kev to 1 Mev. Comparing his tabulated results for the total absorption coefficients of H, C, Al, Cu, Sn, and Pb with our curves for the total absorption coefficients of these elements, we find excellent agreement for all except Sn and Pb. For these elements our values of the total absorption coefficients are greater than his by 10 to 15 percent.

Gray's[20] empirical equation

$$\log_{10}\tau=\bar{3}.6505+1.0\log_{10}\lambda+0.480(\log_{10}\lambda)^2, \quad (41)$$

where τ is in cm^{-1} and λ is in X-units (10^{-11} cm), has been considered the best available for the γ-ray region and values from it have been assumed to be accurate within about 10 percent. A comparison with values obtained from Figs. 13 to 17 shows that the results from Eq. (41) agree with the theoretical ones within 10 percent up to energies of about 1.5 Mev. At higher energies the values given by Eq. (41) are too low by an ever increasing factor.

6. Variation with Atomic Number Z

From log-log plots of ${}_a\tau$ *vs* Z it is found that according to the theory the variation of ${}_a\tau$ with Z does not follow a simple power law, although for practical purposes the deviation from a power law is small. The exponent giving the best agreement with theory increases with γ-ray energy and is between 4 and 5 for energies above 0.35 Mev, being approximately 4.5 at 1.13 Mev and 4.6 at 2.62 Mev.

7. Variation with Wavelength

The variation of ${}_a\tau$ with wavelength is shown in Fig. 18 where ${}_a\tau/Z^5$ is plotted against n (which is proportional to λ). Curves are given for various atomic numbers. Lines marked λ, λ^2, and λ^3 indicate the slopes expected if ${}_a\tau$ varied as λ, λ^2, or λ^3. Two things are ap-

[20] L. H. Gray, Proc. Cambridge Phil. Soc. **27**, 103 (1931).

parent from these curves: (1) The variation of ${}_a\tau$ with λ changes continuously as the wavelength increases (or energy decreases). (2) In a given energy range the variation of ${}_a\tau$ with λ is different for different Z, varying for low Z as a higher power of λ than for high Z.

8. Angular Distribution of Photoelectrons[21]

The photoelectrons produced by γ-rays are not all emitted in the same direction nor is their directional distribution isotropic. To a first approximation one may consider that at low energies the emission is due entirely to the electric vector of the incident wave acting on the electron. If one assumes that the electron goes off on the tangent to its atomic orbit and that the probability of its being emitted is proportional to the square of the projection of the electric vector on the direction of its velocity,[22] then the probability per unit solid angle of an electron being emitted at an angle ψ with respect to the electric vector is proportional to $\cos^2\psi$. In terms of the polar coordinates θ and φ (Fig. 19), the intensity is

TABLE X. Photoelectric effect. Numerical values of ${}_a\tau/Z^5n$ used for curves of Figs. 13 to 17 (in units of 10^{-32}).

n	Mev	$Z=0$	$Z=13$	$Z=26$	$Z=38$	$Z=50$	$Z=65$	$Z=82$
0		0.353	0.275	0.228	0.203	0.188	0.166	0.159
0.1	5.108	0.436	0.343	0.289	0.255	0.230	0.206	0.182
0.125	4.086	0.453	0.362	0.306	0.272	0.247	0.216	0.188
0.194	2.633	0.524	0.412	0.347	0.302	0.270	0.237	0.205
0.25	2.043	0.581	0.447	0.375	0.331	0.290	0.259	0.225
0.375	1.362	0.740	0.556	0.462	0.403	0.366	0.319	0.278
0.50	1.022	0.956	0.694	0.575	0.500	0.440	0.397	0.341
0.75	0.6811	1.528	1.162	0.947	0.781	0.690	0.600	0.522
1.0	0.5108	2.375	1.862	1.506	1.237	1.038	0.878	0.747
1.25	0.4086	3.578	2.756	2.188	1.815	1.512	1.262	1.031
1.5	0.3405	5.3	3.834	3.062	2.528	2.116	1.750	1.362
2.0	0.2554	9.48	7.46	5.34	4.24	3.55	2.96	2.17
3.0	0.1703	24.3	17.61	12.44	8.81	7.88	6.25	4.18
4.0	0.1277	46.8	33.1	22.8	14.8	14.2	10.5	6.64
5.0	0.1022	79.9	53.4	34.6	21.8	21.6	15.6	9.61

proportional to $\sin^2\theta\cos^2\varphi$, or

$$dI\sim\sin^2\theta\cos^2\varphi d\Omega,$$

where $d\Omega$ is an elementary solid angle. More rigorous calculations have been made using the wave equations of the electrons. Neglecting relativity and spin corrections, Fischer[16] finds that

$$dI=Jd\Omega\sim\{\sin^2\theta\cos^2\varphi/[1+(h\nu/2mc^2)-\beta\cos\theta]^4\}d\Omega, \quad (42)$$

while Sauter,[14] using relativistic considerations but assuming that $\beta=v/c\sim1$ and that $Z/137\ll1$, obtains

$$dI=Jd\Omega\sim\beta^2\sin^2\theta\left\{\frac{(1-\beta^2)^{\frac{1}{2}}\cos^2\varphi}{(1-\beta\cos\theta)^4}-\frac{[1-(1-\beta^2)^{\frac{1}{2}}]\cos^2\varphi}{2(1-\beta^2)^{\frac{1}{2}}(1-\beta\cos\theta)^3}+\frac{[1-(1-\beta^2)^{\frac{1}{2}}]^2}{4(1-\beta^2)(1-\beta\cos\theta)^3}\right\}d\Omega. \quad (43)$$

[21] Another analysis, using a different approach and including approximations is given by C. Morette, J. phys. et radium **7**, 135 (1946).

[22] P. Auger and F. Perrin, Compt. rend. **180**, 1742 (1925).

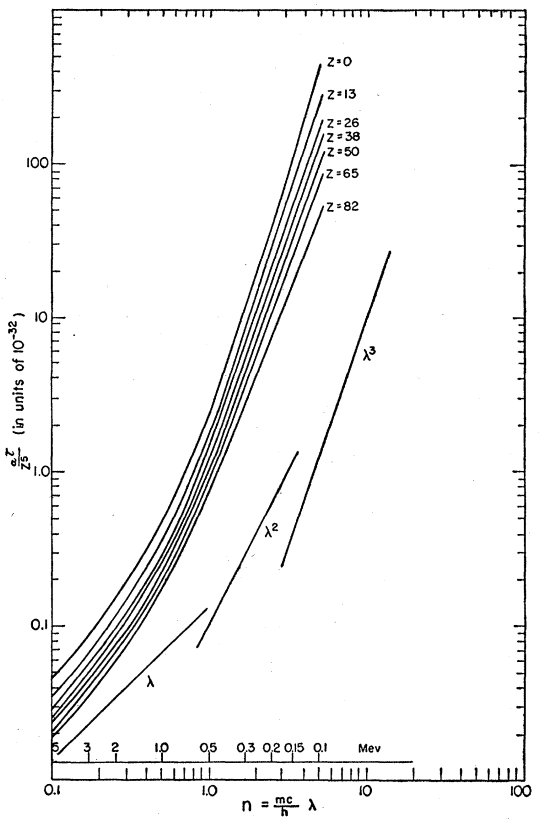

FIG. 18. Photoelectric effect. Variation of cross section with wavelength. Lines marked λ, λ^2, and λ^3 indicate slopes expected if ${}_a\tau$ varied as λ, λ^2, or λ^3.

The terms $(1-\beta\cos\theta)^4$ and $(1-\beta\cos\theta)^3$ in the denominators of these more rigorously calculated equations show that as the energy of the γ-rays is increased, more and more of the photoelectrons are emitted in a forward direction. Hulme[15] has also made relativistic calculations (Table XI) but does not obtain an answer in terms of an equation. His results are presented as the numerical values of the ratio of the average forward momentum of the photoelectrons to the photon momentum, for different values of photon energy (see Fig. 23).

An experimental study of the angular distribution of photoelectrons may yield one of various quantities, depending on the particular method used. The more common quantities are (1) the ratio of the number of photoelectrons emitted in a forward direction, to those emitted in a backward direction; (2) the bipartition angle or the half-angle of a cone, such that half the photoelectrons are emitted within the cone, the other

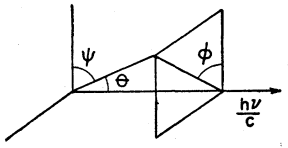

FIG. 19. Photoelectric effect. Angular notation.

TABLE XI. Photoelectric effect. R=ratio of the average forward momentum of the photoelectrons to the photon momentum, as given by Hulme (reference 15).

Mev	λ (in 10^{-10} cm)	R
$\rightarrow\infty$	$\rightarrow 0$	1.0
1.022	1.22	1.15
0.5108	2.43	1.29
0.2043	6.08	1.48
0.1277	9.73	1.57
$\rightarrow 0$	$\rightarrow\infty$	1.6

half outside it; (3) the average value of $\cos\theta$, which is directly related to the average forward momentum of the photoelectrons through the relation[15]

$$R=\frac{\text{Av p. e. forward momentum}}{\text{photon momentum}}=\left(1+\frac{2mc^2}{h\nu}\right)^{\frac{1}{2}}(\cos\theta)_{\text{Av}}, \quad (44)$$

if binding energies are neglected; and (4) an actual differential distribution, i.e., in cloud-chamber measurements the number of photoelectrons emitted between the two cones of half angles θ and $\theta+d\theta$ or in counter measurements the number emitted in the solid angle subtended by the counter at the source.

To compare the theories with experiment, therefore, it is necessary to obtain the theoretical expressions for the above quantities. Putting $d\Omega=\sin\theta d\theta d\varphi$, we find the number emitted within a cone of half angle θ is proportional to

$$\int dI\sim\int_0^{\theta}\left(\int_0^{2\pi}Jd\varphi\right)\sin\theta d\theta. \quad (45)$$

The ratio of forward to backward emitted photoelectrons is therefore

$$\frac{N_{\text{for.}}}{N_{\text{back.}}}=\frac{\int_0^{\pi/2}\left(\int_0^{2\pi}Jd\varphi\right)\sin\theta d\theta}{\int_0^{\pi}\left(\int_0^{2\pi}Jd\varphi\right)\sin\theta d\theta-\int_0^{\pi/2}\left(\int_0^{2\pi}Jd\varphi\right)\sin\theta d\theta}, \quad (46)$$

while the bipartition angle is obtained from the equation

$$\frac{\int_0^{\theta}\left(\int_0^{2\pi}Jd\varphi\right)\sin\theta d\theta}{\int_0^{\pi}\left(\int_0^{2\pi}Jd\varphi\right)\sin\theta d\theta}=\tfrac{1}{2}. \quad (47)$$

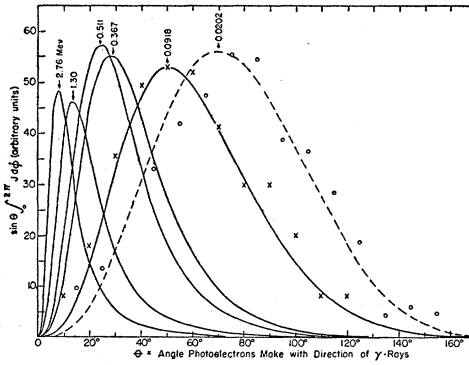

FIG. 20. Photoelectric effect. Directional distribution of photoelectrons for different energies, applicable to cloud-chamber measurements. *Solid curves:* calculated using Sauter's relativistic Eq. (52). *Dashed curve:* calculated using Fischer's nonrelativistic Eq. (51) but using relativistic $\beta=v/c$. *Crosses:* measured values of E. Lutze at 0.0918 Mev (Ann. Physik **9**, 853 (1931)). *Circles:* measured values of Williams, Nuttall, and Barlow at 0.0202 Mev (Proc. Roy. Soc. (London) **121A**, 611 (1928)).

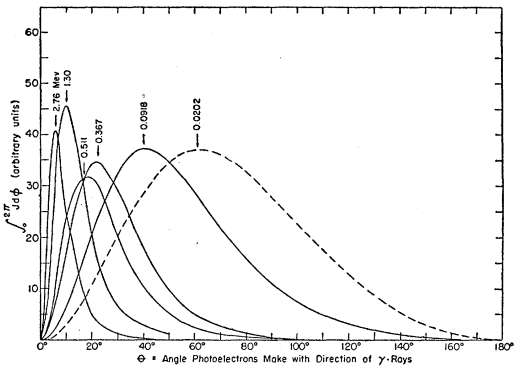

FIG. 21. Photoelectric effect. Directional distribution of photoelectrons for different energies, applicable to counter measurements. *Solid curves:* calculated using Sauter's relativistic Eq. (52). *Dashed curve:* calculated using Fischer's nonrelativistic Eq. (51) but using relativistic $\beta=v/c$.

The average value of $\cos\theta$ is given by

$$(\cos\theta)_{\text{Av}}=\frac{\int_0^{\pi}\left(\int_0^{2\pi}Jd\varphi\right)\cos\theta\sin\theta d\theta}{\int_0^{\pi}\left(\int_0^{2\pi}Jd\varphi\right)\sin\theta d\theta}. \quad (48)$$

For the differential distribution we note that the number emitted between the two cones of half angle θ and $\theta+d\theta$ is just the integral with respect to φ of $Jd\Omega$, i.e.,

$$\sin\theta d\theta\int_0^{2\pi}Jd\varphi. \quad (49)$$

It is this value, as a function of θ, which is obtained from cloud-chamber measurements. In experiments with a counter where measurements are made on only one plane, the angle which the plane makes with the direc-

tion of polarization must be known, and in comparing theory with experiment the particular value of φ being studied must be used in place of the integral with respect to φ. In most cases, however, the radiation is not polarized, so the intensity on any plane is the sum of the intensities on that plane due to all polarizations, and is the same for all values of φ. If $d\omega$ is the solid angle subtended by the counter at the source, the fraction of all the photoelectrons emitted between θ and $\theta+d\theta$ which the counter intercepts is $d\omega/(2\pi\sin\theta d\theta)$. Therefore the intensity as a function of θ when measured by a counter is proportional to

$$(d\omega/\sin\theta d\theta)\sin\theta d\theta\int_0^{2\pi}Jd\varphi=d\omega\int_0^{2\pi}Jd\varphi. \quad (50)$$

It is of interest to calculate the theoretical values of these various quantities for different energies of the incident photons.[23] Integrating with respect to φ from 0 to 2π, we have, using Fischer's Eq. (42),

$$\int_0^{2\pi}Jd\varphi=\text{const}\times\sin^2\theta/[1+(h\nu/2\,mc^2)-\beta\cos\theta]^4 \quad (51)$$

and using Sauter's Eq. (43),

$$\int_0^{2\pi}Jd\varphi=\text{const}\times\beta^2\sin^2\theta\left\{\frac{(1-\beta^2)^{\frac{1}{2}}}{(1-\beta\cos\theta)^4}-\frac{[1-(1-\beta^2)^{\frac{1}{2}}]}{2(1-\beta^2)^{\frac{1}{2}}(1-\beta\cos\theta)^3}+\frac{2[1-(1-\beta^2)^{\frac{1}{2}}]}{4(1-\beta^2)(1-\beta\cos\theta)^3}\right\}. \quad (52)$$

The distribution as obtained with counter measurements should be given by these equations in the energy regions for which each is valid. For the distribution obtained in a cloud chamber, these equations should be multiplied by $\sin\theta$. Curves for these two distributions ($\sin\theta\int_0^{2\pi}Jd\varphi$ and $\int_0^{2\pi}Jd\varphi$) are given in Figs. 20 and 21, respectively, for different energies of the incident photons. These curves have not been normalized and show only the relative distribution for each energy.

To calculate the other three quantities of interest, i.e., the ratio of forward to backward emitted photoelectrons, the bipartition angle, and $(\cos\theta)_{Av}$, integrations have been carried out graphically, with the results shown in Figs. 22 and 23. In Fig. 22 is plotted, as a function of θ, the quantity

$$N_\theta=\frac{\int_0^\theta\left(\int_0^{2\pi}Jd\varphi\right)\sin\theta d\theta}{\int_0^\pi\left(\int_0^{2\pi}Jd\varphi\right)\sin\theta d\theta}, \quad (53)$$

[23] The equations, being functions of the electron velocities, depend on the ionization potential of the absorber, i.e., on its atomic number, as well as on the photon energy. However, except for photons of very low energies (<50 kev) the ionization potential is negligible compared with the photon energy. So unless otherwise specified the numerical calculations given later neglect the ionization potential, i.e., they are for $Z=0$.

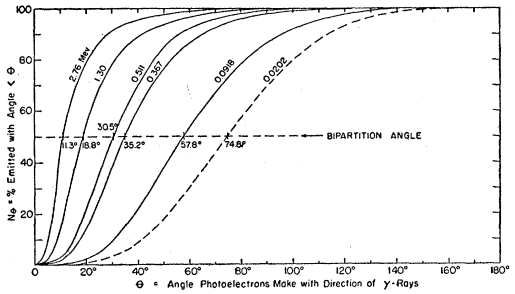

FIG. 22. Photoelectric effect. The fraction of photoelectrons emitted within the cone of half-angle θ for different energies. Bipartition angle is that at which this fraction is 50 percent. *Solid curves:* calculated using Sauter's relativistic Eq. (52). *Dashed curve:* calculated using Fischer's nonrelativistic Eq. (51) with relativistic $\beta=v/c$.

i.e., the fraction of the photoelectrons emitted within the cone of half angle θ. The value of θ at $N_\theta=\frac{1}{2}$ is the bipartition angle, while the ratio of $N_{90°}$ to $N_{180°}-N_{90°}$ is the ratio of the number of forward to the number of backward emitted electrons. In Fig. 23 are plotted, as a function of photon energy, (1) the bipartition angle obtained from Fig. 22; (2)$(\cos\theta)_{Av}$ as obtained from graphical integration of the curve of $\cos\theta\sin\theta\int_0^{2\pi}Jd\varphi$ *vs* θ and also as calculated from Hulme's values of R and Eq. (44); and (3) the ratio R of the average forward momentum to the photon momentum, as given by Hulme and as calculated from $(\cos\theta)_{Av}$ obtained with Sauter's equations.

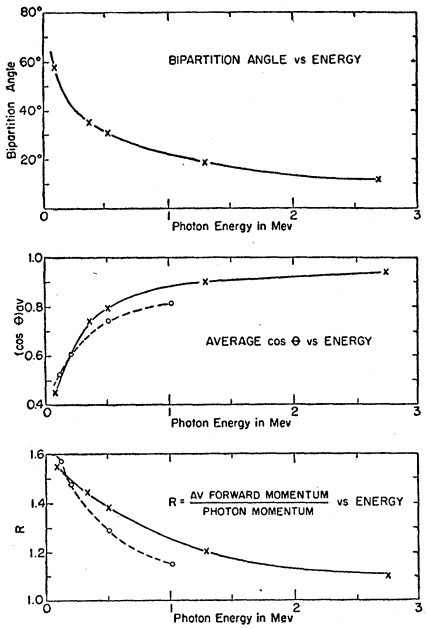

FIG. 23. Photoelectric effect. (1) Values of bipartition angles obtained from Fig. 22. (2) Values of $(\cos\theta)_{Av}$ obtained from graphical integration of curves of $\cos\theta\sin\theta\int_0^{2\pi}Jd\varphi$ *vs* θ using Sauter's Eq. (52) (crosses and solid curve); also from Hulme's values of R, Table XI and Eq. (44) (circles and dashed curve). (3) Values of R as given by Hulme (circles and dashed curve) and as calculated with Eq. (44) from $(\cos\theta)_{Av}$ obtained with Sauter's equations (crosses and solid curve).

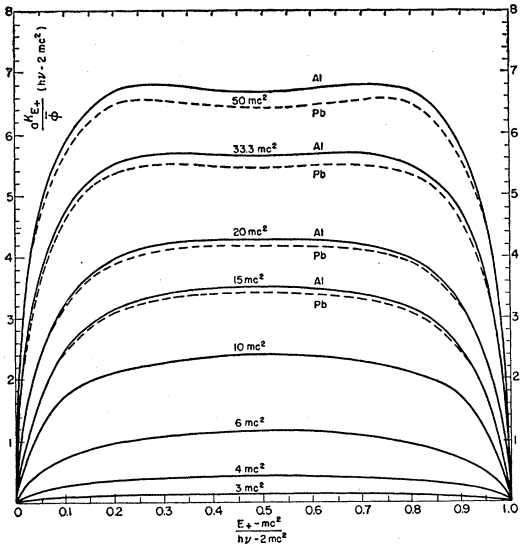

FIG. 24. Pair production. Energy distribution of pairs. ${}_a\kappa_{E_+}dE_+$ is the cross section for the creation of a positive electron with an energy between E_+ and $E_+ + dE_+$. For energies up to 10 mc^2 Eq. (59) was used. Curves for higher energies were calculated for Pb and Al from Eqs. (60) and (61).

The values given in Figs. 22 and 23 were obtained by graphical integration. The integration can, however, be carried out analytically. To do this Eq. (51) or (52) is inserted in the quantity wanted [Eqs. (45), (46), (47), (48), (49), or (50)]. The integrals involved are the following:

$$\int_0^\theta \frac{\sin^3\theta d\theta}{(a-\beta\cos\theta)^4} = \frac{3\beta^2\cos^2\theta - 3a\beta\cos\theta + a^2 - \beta^2}{3\beta^3(a-\beta\cos\theta)^3} - \frac{a-2\beta}{3\beta^3(a-\beta)^2} = \frac{4}{3(a^2-\beta^2)^2} \quad \text{if} \quad \theta=\pi \tag{54}$$

$$\int_0^\pi \frac{\cos\theta\sin^3\theta d\theta}{(a-\beta\cos\theta)^4} = \frac{1}{\beta^4}\ln\frac{a+\beta}{a-\beta} - \frac{2a(3a^2-5\beta^2)}{3\beta^3(a^2-\beta^2)^2} \tag{55}$$

$$\int_0^\theta \frac{\sin^3\theta d\theta}{(1-\beta\cos\theta)^3} = \frac{\beta^2-4\beta+3}{2\beta^3(1-\beta)^2} - \frac{\beta^2+3-4\beta\cos\theta}{2\beta^3(1-\beta\cos\theta)^2} - \frac{1}{\beta^3}\ln\frac{1-\beta\cos\theta}{1-\beta} = \frac{2}{\beta^2(1-\beta^2)} - \frac{1}{\beta^3}\ln\frac{1+\beta}{1-\beta} \quad \text{if} \quad \theta=\pi \tag{56}$$

$$\int_0^\pi \frac{\cos\theta\sin^3\theta d\theta}{(1-\beta\cos\theta)^3} = \frac{2(3-2\beta^2)}{\beta^3(1-\beta^2)} - \frac{3}{\beta^4}\ln\frac{1+\beta}{1-\beta}, \tag{57}$$

where $a=1+h\nu/2\,mc^2$. A particularly simple result is obtained when Eq. (51) is inserted in (46). Then

$$\frac{N_{\text{for.}}}{N_{\text{back.}}} = \frac{(2a-\beta)(a+\beta)^2}{(2a+\beta)(a-\beta)^2}. \tag{58}$$

PAIR PRODUCTION

At energies greater than 2 mc^2, i.e., greater than 1.02 Mev, absorption of γ-rays by the process of pair production must be considered. In this process the energy of a photon reacting with the field of a nucleus is converted into a positive and a negative electron each of mass m, the remaining energy going into the kinetic energy of the two particles. A theoretical analysis of this process has been made by Bethe and Heitler,[24] which involves a consideration of the negative states of an electron. Using the Born approximation, in which the interaction between the electron and the nucleus is considered a small perturbation, and keeping only the first terms,[25] the following equation is obtained for the cross section for the creation of a positron with total energy between E_+ and $E_+ + dE_+$ and a negatron with total energy between E_- and $E_- - dE_-$:

$$\begin{aligned} {}_a\kappa_{E_+}dE_+ = \phi\frac{p_+p_-}{(h\nu)^3}dE_+\Big\{ &-\frac{4}{3} - 2E_+E_-\frac{p_+^2+p_-^2}{p_+^2p_-^2} \\ &+ mc^2\left(\frac{E_+\epsilon_-}{p_-^3} + \frac{\epsilon_+E_-}{p_+^3} - \frac{\epsilon_+\epsilon_-}{p_+p_-}\right) \\ &+ L\left[\frac{(h\nu)^2}{p_+^3p_-^3}(E_+^2E_-^2+p_+^2p_-^2) - \frac{8}{3}\frac{E_+E_-}{p_+p_-}\right. \\ &- \frac{m^2c^4h\nu}{2p_+p_-}\left(\frac{E_+E_--p_-^2}{p_-^3}\epsilon_- \right. \\ &\left.\left. + \frac{E_+E_--p_+^2}{p_+^3}\epsilon_+ + \frac{2h\nu E_+E_-}{p_+^2p_-^2}\right)\right]\Big\}. \end{aligned} \tag{59}$$

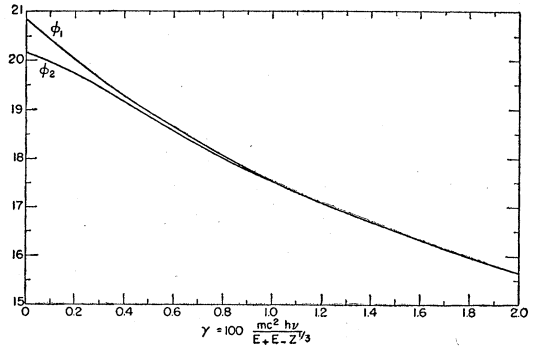

FIG. 25. Pair production. Functions φ_1 and φ_2 for use in Eq. (60). From Bethe and Heitler (reference 24).

[24] H. Bethe and W. Heitler, Proc. Roy. Soc. (London) **146A**, 83 (1934).

[25] Reference 18, p. 83, footnote.

Here

$$E_-=h\nu-E_+,$$
$$\epsilon_+=2\ln[(E_++p_+)/mc^2],$$
$$\epsilon_-=2\ln[(E_-+p_-)/mc^2],$$
$$L=2\ln[(E_+E_-+p_+p_-+m^2c^4)/mc^2h\nu],$$
$$\tilde{\phi}=Z^2r_0^2/137,$$

p_+ and p_- are the momenta of the electrons in energy units, and the other symbols are the same as defined above. The total cross section, i.e., the cross section for the production of a positive and negative electron pair, is obtained by integrating Eq. (59) over all possible energies of the positive electron. Analytical integration of Eq. (59) is impossible, but the total cross section for a given energy can be obtained from the area under the curves in Fig. 24. Here the abscissas are the fraction of the available kinetic energy which the positron receives. In order that the area under the curves be the total cross section, the ordinates are the values of ${}_{a\kappa}E_+$ in units of $\tilde{\phi}$, multiplied by the total kinetic energy, $h\nu-2\,mc^2$. The curves for $3\,mc^2$, $4\,mc^2$, $6\,mc^2$, and $10\,mc^2$ were obtained from Eq. (59).[26]

At energies greater than $10\,mc^2$ Eq. (59) is not valid, since at high energies it becomes more and more probable that the electron pair will be formed some distance from the nucleus. When the distance from the nucleus at which pair production is most probable lies outside some of the electronic shells of the atom, the field in which the pairs are created is less than that of the nucleus alone, by a factor depending on the atomic form factor. Calculations taking this into consideration have been made by Bethe.[27] He obtains as the cross section for the creation of a positive electron with total energy between E_+ and E_++dE_+, the equation

$$ {}_{a\kappa}E_+dE_+=[\tilde{\phi}/(h\nu)^3]dE_+ \times\{(E_+^2+E_-^2)[\varphi_1(\gamma)-(4/3)\ln Z] +(2/3)E_+E_-[\varphi_2(\gamma)-(4/3)\ln Z]\}, \quad (60)$$

where $\gamma=(100\ mc^2\ h\nu)/(E_+E_-Z^{\frac{1}{3}})$ and φ_1 and φ_2 are functions of γ whose values were obtained by numerical integration. Curves of φ_1 and φ_2, taken from Bethe and Heitler,[24] are reproduced here in Fig. 25. For smaller energies ($2<\gamma<15$) a more convenient formula[24] is

$$ {}_{a\kappa}E_+dE_+=[\tilde{\phi}/(h\nu)^3]dE_+[E_+^2+E_-^2+(2/3)E_+E_-]4 \times[\ln(2E_+E_-/h\nu\,mc^2)-(1/2)-c(\gamma)]. \quad (61)$$

Values of $c(\gamma)$ given by Bethe and Heitler are plotted in Fig. 26. The curves of Fig. 24 for energies above $10\,mc^2$ were calculated for Pb and Al by use of Eqs. (60) and (61).[26]

The total cross sections for pair production are obtained by measuring the areas under the curves of Fig. 24. These are given in Table XII and are plotted in Fig. 27.

At very low photon energies the above equations for pair production cross sections do not give the correct result, since at low energies the Born approximation does not hold, i.e., the interaction between the electrons and the nucleus is not negligible. Because of the repulsion of the positron and the attraction of the negatron to the nucleus the energy distribution is not symmetrical. Calculations including the interactions between the electrons and the nucleus have been made by Jaeger and Hulme.[28] Their results are in the form of numerical values for the photon energies of $3\,mc^2$ (1.53 Mev) and $5.2\,mc^2$ (2.66 Mev). They also calculated $\bar{E}_+-\bar{E}_-$, the difference in the average energies of the positron and negatron, respectively, for the same two photon energies. Their values are given in Table XIII, along with values for the same energies obtained from Eq. (59) of Bethe and Heitler. Jaeger and Hulme estimate the possible

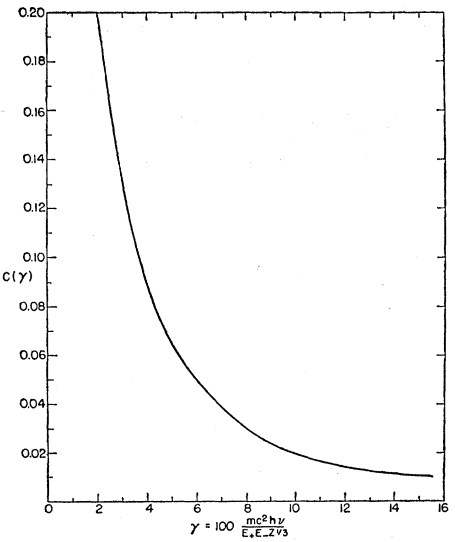

FIG. 26. Pair production. Function $c(\gamma)$ for use in Eq. (61). From Bethe and Heitler (reference 24).

TABLE XII. Pair production cross sections obtained from areas under the curves of Fig. 24.

Mev	${}_{a\kappa}/\tilde{\phi}$		${}_{a\kappa}/Z^2$ (units of 10^{-27} cm²/atom)	
1.533	0.086		0.050	
2.043	0.327		0.189	
3.065	0.905		0.524	
5.108	1.98		1.15	
	Al	Pb	Al	Pb
7.662	2.93	2.86	1.70	1.66
10.22	3.66	3.60	2.12	2.08
17.01	5.07	4.90	2.94	2.84
25.54	6.14	5.96	3.56	3.46

[26] Similar curves, calculated from the same equation are given by B. Rossi and K. Greiser, Revs. Modern Phys. **13**, 240 (1941), as well as by Bethe and Heitler (reference 24) and also by Heitler (reference 25, p. 199). For a comparison of final cross section values see Fig. 27.

[27] H. Bethe, Proc. Cambridge Phil. Soc. **30**, 524 (1934).

[28] J. C. Jaeger and H. R. Hulme, Proc. Roy. Soc. (London) **153A**, 443 (1936).

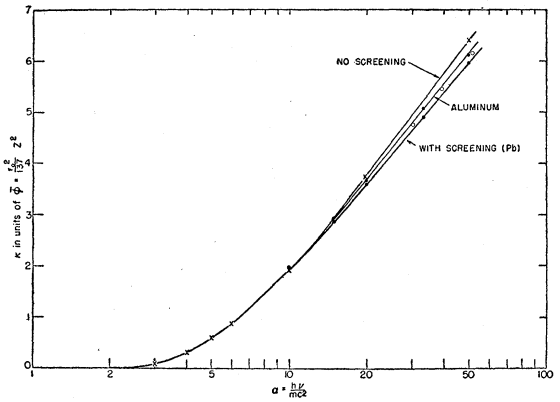

FIG. 27. Pair production. Integrated cross sections *vs* energy. *Solid circles:* values calculated by the authors. *Crosses:* values from Heitler (reference 18, p. 200). *Open circles:* values for Pb from Rossi and Greisen (reference 26).

error in the calculations at 5.3 mc^2 as about 10 percent, the error for 3 mc^2 being somewhat less. At low energies therefore, the more accurate theoretical value for the absorption coefficient may be as much as twice that obtained using the Born approximation. However, at energies of 3 Mev or higher little error is involved in using the Born approximation. Since in most elements the effect of pair production is very much less at these low energies than the Compton effect, we have neglected this correction and used only the results of Bethe and Heitler.

TOTAL ABSORPTION COEFFICIENTS

Using the values for the partial absorption coefficients obtained from the theories for Compton effect, photoelectric effect, and pair production as discussed above, we have calculated the expected values of the total absorption coefficients for different energies and different elements. For each element we used the following procedure:

1. Multiplied the values of Table II by Z to get the total Compton cross section, ${}_a\sigma$.
2. Found the values of ${}_a\tau/Z^5n$ for different values of n, using Figs. 13 to 17, and multiplied each by Z^5n to get ${}_a\tau$.
3. Obtained values for ${}_a\kappa/\bar{\phi}$ from Table XII for the same values of $n(=1/\alpha)$ used in steps 1 and 2, and multiplied these by $\bar{\phi}=5.796\times10^{-28}Z^2$ to obtain ${}_a\kappa$.
4. Obtained ${}_a\mu$ from the sum ${}_a\sigma+{}_a\tau+{}_a\kappa$.

Numerical values of ${}_a\mu$, ${}_a\sigma$, ${}_a\tau$, and ${}_a\kappa$ for some elements are given in Table XIV and are plotted as curves in Figs. 28 to 42. The general features of these curves may be summarized as follows: At very low energies absorption by photoelectrons predominates, but decreases rapidly with increasing energy. As it decreases, absorption by Compton effect becomes relatively more important until in the region of energies slightly less than 1 Mev almost all the absorption is by Compton effect. At energies of about 1-Mev absorption by pair production starts and continues to increase, while the other effects decrease, until at high energies the absorption is almost completely by pair production. The curves of absorption coefficient *vs* energy have, therefore, a minimum at the energies where the Compton effect and pair production become comparable. While these features are characteristic of the absorption curves for all elements, the particular energy at which one mode of absorption or another is important changes from element to element. In carbon, photoelectric absorption is already negligible at 0.1 Mev and pair production is just starting to become important at 10 Mev; while in lead, photoelectric absorption and pair production are both of some importance at 2 Mev. However, in all the elements absorption by the Compton effect predominates in the energy region from about 0.5 Mev to 4 Mev, and it is for this reason that the absorption coefficients, when expressed in cm²/electron or cm²/g show least variation from element to element.

MEASUREMENT OF ABSORPTION COEFFICIENTS

Necessary Considerations

In a few cases the absorption of γ-rays by a single one of the three processes has been studied experimentally.[13,29] However, such experiments require special apparatus for selecting only those secondary particles produced by the particular method of absorption being studied. The simplest method of testing the theory, and that used by most experimenters, is to measure the total absorption coefficients. Although such measurements are fundamentally simple, considerable care must be taken in choosing and arranging the apparatus so that unwanted radiation can either be eliminated from the measurements or be properly accounted for, and so that the results of the experiments can be properly interpreted. This involves knowledge of the energy of the photons emitted from the source, the purity of the absorbers, the efficiency of the detector as a function of photon energy, and the effect of the geometry on the amount of scattered radiation reaching the detector as well as on the path length through the absorber for different rays of the beam.

1. Sources

The comparison of experimental results with theory is simplest when the source used emits photons of only

TABLE XIII. Pair production cross sections and difference in average energy of positrons and negatrons for lead, as calculated by Jaeger and Hulme (reference 28) and compared with results from Bethe and Heitler (reference 24).

Mev	${}_a\kappa$ (units of 10^{-24} cm²/atom) Bethe-Heitler	Jaeger-Hulme	$\bar{E}_+-\bar{E}_-$ Jaeger-Hulme
1.53	0.34	0.67	0.33
2.66	2.6	3.1	0.55

[29] K. Zuber, Helv. Phys. Acta **15**, 38 (1942).

TABLE XIV. Values of absorption coefficients for some of the elements (in units of 10^{-24} cm²/atom).

Mev	$a\sigma$	$a\tau$	$a\kappa$	$a\mu$
Hydrogen $Z=1$				
0.1022	0.4900	Negligible		(Same
0.1277	0.4636	(10^{-30} or less)		as $a\sigma$)
0.1703	0.4273			
0.2554	0.3744			
0.3405	0.3369			
0.4086	0.3140			
0.5108	0.2866			
0.6811	0.2529			
1.022	0.2090			
1.362	0.1806		0.000029	
1.533	0.1696		0.000049	
2.043	0.1446		0.000185	0.1448
2.633	0.1246		0.000371	0.1250
3.065	0.1136		0.000522	0.1141
4.086	0.09465		0.000844	0.09549
5.108	0.08168		0.001124	0.08280
6.130	0.07215		0.001356	0.07351
Carbon $Z=6$				
0.1022	2.940	0.0257		2.966
0.1277	2.781	0.0125		2.793
0.1703	2.564	0.00495		2.569
0.2554	2.247	0.00132		2.248
0.3405	2.022	0.000524		2.023
0.4086	1.884	0.000308		1.884
0.5108	1.719	0.000164		1.719
0.6811	1.517	0.000078		1.517
1.022	1.254	0.000031		1.254
1.362	1.083	0.000019	0.001043	1.084
1.533	1.018		0.001774	1.020
2.043	0.8675	0.000010	0.006677	0.8742
2.633	0.7475	0.000007	0.01335	0.7609
3.065	0.6815		0.01878	0.7003
4.086	0.5679	0.000004	0.03025	0.5981
5.108	0.4901	0.000003	0.04048	0.5306
6.130	0.4329		0.04945	0.4823
Nitrogen $Z=7$				
0.1022	3.430	0.0540		3.484
0.1277	3.245	0.0262		3.271
0.1703	2.991	0.0104		3.001
0.2554	2.621	0.00313		2.624
0.3405	2.358	0.00111		2.359
0.4086	2.198	0.000651		2.199
0.5108	2.005	0.000350		2.005
0.6811	1.770	0.000165		1.770
1.022	1.463	0.0000661		1.463
1.362	1.264	0.0000394	0.001420	1.265
1.533	1.187		0.002414	1.189
2.043	1.012	0.0000209	0.009088	1.021
2.633	0.8721	0.0000145	0.01818	0.8903
3.065	0.7950		0.02556	0.8206
4.086	0.6625	0.0000084	0.04118	0.7037
5.108	0.5718	0.0000064	0.05510	0.6269
6.130	0.5051		0.06646	0.5716
Oxygen $Z=8$				
0.1022	3.920	0.1022		4.022
0.1277	3.709	0.0498		3.759
0.1703	3.418	0.0197		3.438
0.2554	2.996	0.00537		3.001
0.3405	2.695	0.00211		2.697
0.4086	2.512	0.00124		2.513
0.5108	2.293	0.000670		2.294
0.6811	2.023	0.000316		2.023
1.022	1.672	0.000128		1.672
1.362	1.445	0.0000753	0.001855	1.447
1.533	1.357		0.003153	1.360
2.043	1.157	0.0000400	0.01187	1.169
2.633	0.9967	0.0000284	0.02374	1.020
3.065	0.9086		0.03338	0.9420
4.086	0.7572	0.0000162	0.05378	0.8110
5.108	0.6534	0.0000123	0.07196	0.7254
6.130	0.5772		0.08680	0.6640

Mev	$a\sigma$	$a\tau$	$a\kappa$	$a\mu$
Sodium $Z=11$				
0.1022	5.390	0.457		5.847
0.1277	5.099	0.232		5.331
0.1703	4.700	0.0899		4.790
0.2554	4.119	0.0248		4.144
0.3405	3.701	0.0097		3.711
0.4086	3.454	0.0058		3.460
0.5108	3.152	0.0031		3.155
0.6811	2.782	0.0015		2.784
1.022	2.299	0.00058		2.300
1.362	1.986	0.00035	0.00351	1.990
1.533	1.866		0.00596	1.872
2.043	1.590	0.00019	0.02244	1.612
2.633	1.370	0.00013	0.04488	1.415
3.065	1.249		0.06311	1.312
4.086	1.041	0.00008	0.1017	1.143
5.108	0.8985	0.00006	0.1360	1.035
6.130	0.7937		0.1641	0.9578
Magnesium $Z=12$				
0.1022	5.880	0.687		6.567
0.1277	5.563	0.338		5.901
0.1703	5.127	0.135		5.262
0.2554	4.493	0.0374		4.530
0.3405	4.043	0.0147		4.058
0.4086	3.768	0.00872		3.777
0.5108	3.439	0.00476		3.444
0.6811	3.034	0.00221		3.036
1.022	2.508	0.000883		2.509
1.362	2.167	0.000529	0.00417	2.172
1.533	2.035		0.00709	2.042
2.043	1.735	0.000283	0.0267	1.762
2.633	1.495	0.000202	0.0534	1.548
3.065	1.363		0.0751	1.438
4.086	1.136	0.000114	0.121	1.257
5.108	0.9802	0.000087	0.162	1.142
6.130	0.8658		0.198	1.064
Aluminum $Z=13$				
0.1022	6.370	0.991		7.361
0.1277	6.026	0.492		6.518
0.1703	5.555	0.196		5.751
0.2554	4.868	0.0554		4.923
0.3405	4.380	0.0214		4.401
0.4086	4.082	0.0128		4.095
0.5108	3.725	0.00691		3.732
0.6811	3.287	0.00324		3.290
1.022	2.717	0.00129		2.718
1.362	2.347	0.000774	0.00490	2.353
1.533	2.205		0.00833	2.214
2.043	1.880	0.000415	0.0313	1.911
2.633				
3.065	1.476		0.0882	1.564
4.086	1.230	0.000168	0.142	1.372
5.108	1.062	0.000127	0.190	1.252
6.130	0.9380		0.2292	1.167
10.22	0.6525		0.3582	1.011
17.03	0.4451		0.4962	0.9413
25.54	0.3248		0.6016	0.9264
Silicon $Z=14$				
0.1022	6.860			
0.1277	6.490	0.693		7.183
0.1703	5.982	0.278		6.260
0.2554	5.242	0.0774		5.319
0.3405	4.717	0.0305		4.747
0.4086	4.396	0.0182		4.414
0.5108	4.012	0.00984		4.022
0.6811	3.540	0.00460		3.545
1.022	2.926	0.00184		2.928
1.362	2.528	0.00110	0.00568	2.535
1.533	2.374		0.00966	2.385
2.043	2.024	0.000592	0.0364	2.061
2.633	1.744	0.000422	0.0727	1.817
3.065	1.590		0.1022	1.692
4.086	1.325	0.000240	0.1647	1.490
5.108	1.144	0.000181	0.2204	1.364
6.130	1.010		0.2658	1.276
10.22	0.7026			

TABLE XIV.—*Continued.*

Mev	$a\sigma$	$a\tau$	$a\kappa$	$a\mu$
		Chlorine $Z=17$		
0.1022	8.329	2.65		10.98
0.1277	7.881	1.68		9.56
0.1703	7.264	0.675		7.949
0.2554	6.365	0.189		6.554
0.3405	5.728	0.0759		5.804
0.4086	5.337	0.0453		5.382
0.5108	4.871	0.0247		4.896
0.6811	4.299	0.0124		4.311
1.022	3.553	0.00462		3.558
1.362	3.070	0.00277	0.00838	3.081
1.533	2.883		0.0142	
2.043	2.458	0.00149	0.0536	2.513
2.633	2.118	0.00106	0.1072	2.226
3.065	1.931		0.1507	
4.086	1.609	0.00061	0.2429	1.853
5.108	1.389	0.00046	0.3249	1.714
6.130	1.227		0.3919	1.619
		Argon $Z=18$		
0.1022	8.819	4.33		13.15
0.1277	8.344	2.17		10.51
0.1703	7.691	0.870		8.561
0.2554	6.740	0.245		6.985
0.3405	6.065	0.0995		6.164
0.4086	5.651	0.0593		5.710
0.5108	5.158	0.0324		5.190
0.6811	4.552	0.0152		4.567
1.022	3.762	0.00605		3.768
1.362	3.250	0.00364	0.00939	3.263
1.533	3.052		0.0160	
2.043	2.602	0.00196	0.0601	2.664
2.633	2.243	0.00140	0.1202	2.364
3.065	2.044		0.1690	2.214
4.086	1.704	0.000796	0.2723	1.977
5.108	1.470	0.000602	0.3643	1.835
6.130	1.299		0.4394	1.739
		Potassium $Z=19$		
0.1022	9.309	5.47		14.78
0.1277	8.808	2.76		11.57
0.1703	8.118	1.114		9.232
0.2554	7.114	0.313		7.427
0.3405	6.401	0.128		6.529
0.4086	5.965	0.0761		6.041
0.5108	5.445	0.0417		5.487
0.6811	4.804	0.0195		4.824
1.022	3.971	0.0078		3.979
1.362	3.431	0.0047	0.0105	3.446
1.533	3.223		0.0178	3.244
2.043	2.747	0.0025	0.0670	2.816
2.633	2.367	0.0018	0.1339	2.503
3.065	2.158		0.1883	2.348
4.086	1.798	0.0010	0.3034	2.102
5.108	1.552	0.00078	0.4059	1.959
6.130	1.371		0.4896	1.861
		Calcium $Z=20$		
0.1022	9.799	6.89		16.69
0.1277	9.271	3.47		12.74
0.1703	8.546	1.402		9.948
0.2554	7.489	0.395		7.884
0.3405	6.738	0.163		6.901
0.4086	6.279	0.0968		6.376
0.5108	5.731	0.0531		5.784
0.6811	5.057	0.0248		5.082
1.022	4.180	0.0099		4.190
1.362	3.612	0.0060	0.0116	3.630
1.533	3.392		0.0198	
2.043	2.893	0.0032	0.0742	2.970
2.633	2.492	0.0023	0.1484	2.642
3.065	2.272		0.2086	2.483
4.086	1.893	0.0013	0.3362	2.230
5.108	1.634	0.00099	0.4498	2.085
6.130	1.443		0.5425	1.986

Mev	$a\sigma$	$a\tau$	$a\kappa$	$a\mu$
		Manganese $Z=25$		
0.1022	12.25	18.0		30.2
0.1277	11.59	9.30		20.89
0.1703	10.68	3.75		14.43
0.2554	9.361	1.07		10.44
0.3405	8.423	0.456		8.879
0.4086	7.849	0.272		8.121
0.5108	7.164	0.149		7.313
0.6811	6.322	0.0702		6.392
1.022	5.225	0.0283		5.253
1.362	4.514	0.0171	0.0181	4.549
1.533	4.240		0.0308	
2.043	3.614	0.0093	0.1159	3.739
2.633	3.115	0.0066	0.2318	3.354
3.065	2.839		0.3260	
4.086	2.366	0.0038	0.5252	2.895
5.108	2.042	0.0029	0.7027	2.748
6.130	1.804		0.8476	2.654
		Iron $Z=26$		
0.1022	12.74	20.5		33.28
0.1277	12.05	10.8		22.9
0.1703	11.11	4.43		15.54
0.2554	9.735	1.27		11.00
0.3405	8.760	0.546		9.306
0.4086	8.163	0.325		8.488
0.5108	7.451	0.190		7.641
0.6811	6.574	0.0844		6.658
1.022	5.434	0.0342		5.468
1.362	4.695	0.0206	0.0196	4.736
1.533	4.410	0.0170	0.0333	4.460
2.043	3.759	0.0111	0.1254	3.895
2.633				
3.065	2.953	0.00640	0.3526	3.312
4.086	2.461	0.00455	0.5681	3.034
5.108	2.124		0.7601	2.89
6.130	1.876		0.9168	2.79
		Cobalt $Z=27$		
0.1022	13.23	23.7		36.9
0.1277	12.52	13.0		25.5
0.1703	11.54	5.29		16.83
0.2554	10.11	1.52		11.63
0.3405	9.097	0.646		9.743
0.4086	8.477	0.386		8.863
0.5108	7.737	0.211		7.948
0.6811	6.827	0.0998		6.927
1.022	5.643	0.0407		5.684
1.362	4.875	0.0245	0.0211	4.920
1.533	4.579		0.0359	
2.043	3.903	0.0133	0.1352	4.051
2.633	3.364	0.0095	0.2704	3.644
3.065	3.067		0.3803	
4.086	2.555	0.0054	0.6126	3.173
5.108	2.205	0.0041	0.8197	3.029
6.130	1.948		0.9887	
		Copper $Z=29$		
0.1022	14.20	32.5		46.7
0.1277	13.44	17.8		31.2
0.1703	12.39	7.20		19.59
0.2554	10.86	2.07		12.93
0.3405	9.771	0.889		10.66
0.4086	9.105	0.5351		9.640
0.5108	8.310	0.292		8.602
0.6811	7.333	0.138		7.471
1.022	6.061	0.0567		6.118
1.362	5.236	0.0343	0.0244	5.295
1.533	4.919		0.0414	
2.043	4.193	0.0186	0.1560	4.368
2.633	3.613	0.0133	0.3120	3.938
3.065	3.294		0.4387	
4.086	2.745	0.00762	0.7068	3.459
5.108	2.369	0.00572	0.9456	3.320
6.130	2.092		1.141	

TABLE XIV.—*Continued.*

Mev	$a\sigma$	$a\tau$	$a\kappa$	$a\mu$
		Zinc $Z=30$		
0.1022	14.70	39.0		53.7
0.1277	13.91	20.7		34.6
0.1703	12.82	8.38		21.20
0.2554	11.23	2.39		13.62
0.3405	10.11	1.04		11.15
0.4086	9.419	0.623		10.04
0.5108	8.597	0.341		8.938
0.6811	7.586	0.161		7.747
1.022	6.270	0.0662		6.336
1.362	5.417	0.0402	0.0261	5.483
1.533	5.088		0.0443	
2.043	4.337	0.0218	0.1669	4.526
2.633	3.738	0.0156	0.3338	4.088
3.065	3.407		0.4694	
4.086	2.839	0.00893	0.7564	3.604
5.108	2.450	0.00672	1.012	3.469
6.130	2.165		1.221	
		Silver $Z=47$		
0.1022	23.03	260		283
0.1277	21.79	137		159
0.1703	20.08	57.2		77.3
0.2554	17.60	16.9		34.5
0.3405	15.84	7.62		23.46
0.4086	14.76	4.53		19.29
0.5108	13.47	2.48		15.95
0.6811	11.88	1.22		13.10
1.022	9.824	0.520		10.34
1.362	8.487	0.321	0.0640	8.872
1.533	7.972		0.1088	
2.043	6.795	0.172	0.4097	7.377
2.633	5.856	0.123	0.8194	6.799
3.065	5.338		1.152	
4.086	4.448	0.0720	1.856	6.376
5.108	3.839	0.0541	2.484	6.377
6.130	3.391		2.996	
		Tin $Z=50$		
0.1022	24.50	338		362
0.1277	23.18	176		199
0.1703	21.36	74.1		95.5
0.2554	18.72	22.2		40.9
0.3405	16.85	9.92		26.77
0.4086	15.70	5.91		21.61
0.5108	14.33	3.24		17.57
0.6811	12.64	1.62		14.26
1.022	10.45	0.688		11.14
1.362	9.028	0.429	0.0724	9.529
1.533	8.480	0.353	0.1232	8.956
2.043	7.229	0.227	0.4637	7.920
2.633				
3.065	5.679	0.134	1.304	7.117
4.086	4.732	0.0964	2.101	6.929
5.108	4.084	0.0720	2.811	6.967
6.130	3.608	0.0581	3.391	7.057
		Barium $Z=56$		
0.1022	27.44	520		547
0.1277	25.96	278		304
0.1703	23.93	119		143
0.2554	20.97	36.4		57.4
0.3405	18.87	16.2		35.1
0.4086	17.58	9.64		27.22
0.5108	16.05	5.30		21.35
0.6811	14.16	2.68		16.84
1.022	11.70	1.16		12.86
1.362	10.11	0.708	0.0909	10.91
1.533	9.498		0.1545	
2.043	8.097	0.381	0.5816	9.060
2.633	6.977	0.274	1.163	8.414
3.065	6.360		1.636	
4.086	5.300	0.160	2.635	8.095
5.108	4.574	0.121	3.526	8.221
6.130	4.041		4.253	

Mev	$a\sigma$	$a\tau$	$a\kappa$	$a\mu$
		Tantalum $Z=73$		
0.1022	35.77	1288		1324
0.1277	33.84	696		730
0.1703	31.19	326		357
0.2554	27.33	106		133
0.3405	24.60	48.2		72.8
0.4086	22.92	29.7		52.6
0.5108	20.92	16.7		37.6
0.6811	18.46	8.75		27.21
1.022	15.26	3.79		19.05
1.362	13.18	2.32	0.1544	15.65
1.533	12.38		0.2625	
2.043	10.55	1.25	0.9883	12.79
2.633	9.095	0.893	1.977	11.96
3.065	8.291		2.780	
4.086	6.909	0.521	4.478	11.91
5.108	5.963	0.402	5.991	12.36
6.130	5.267		7.227	
		Platinum $Z=78$		
0.1022	38.22	1501		1539
0.1277	36.16	820		856
0.1703	33.33	390		423
0.2554	29.21	139		168
0.3405	26.28	62.6		88.9
0.4086	24.49	39.0		63.5
0.5108	22.35	22.2		44.6
0.6811	19.72	11.9		31.6
1.022	16.30	5.10		21.4
1.362	14.08	3.10	0.1763	17.4
1.533	13.23		0.2997	
2.043	11.28	1.67	1.128	14.08
2.633	9.718	1.19	2.257	13.16
3.065	8.859		3.173	
4.086	7.382	0.696	5.113	13.19
5.108	6.371	0.540	6.840	13.75
6.130	5.628		8.251	
		Lead $Z=82$		
0.1022	40.18	1782		1822
0.1277	38.01	985		1023
0.1703	35.04	465		500
0.2554	30.70	161		192
0.3405	27.63	75.7		103.3
0.4086	25.74	47.8		73.5
0.5108	23.50	27.7		51.2
0.6811	20.73	14.5		35.2
1.022	17.14	6.31		23.45
1.362	14.81	3.86	0.1948	18.87
1.533	13.91		0.3313	
2.043	11.86	2.08	1.247	15.19
2.633				
3.065	9.313		3.507	
4.086	7.761	0.869	5.651	14.28
5.108	6.698	0.675	7.560	14.93
6.130	5.917		9.119	
10.22	4.115	0.316	14.04	18.47
15.32	3.042	0.206	18.00	21.25
25.54	2.044	0.122	23.24	25.41
		Bismuth $Z=83$		
0.1022	40.67	1832		1873
0.1277	38.48	1016		1054
0.1703	35.46	484.5		520
0.2554	31.08	165.4		196.5
0.3405	27.96	79.77		107.7
0.4086	26.06	50.22		76.28
0.5108	23.78	29.15		52.93
0.6811	20.99	15.36		36.35
1.022	17.35	6.696		24.05
1.362	14.99	4.077	0.1996	19.27
1.533	14.08		0.3394	
2.043	12.00	2.206	1.278	15.49
2.633	10.34	1.551	2.555	14.45
3.065	9.427		3.593	
4.086	7.856	0.9158	5.790	14.56
5.108	6.780	0.7130	7.746	15.24
6.130	5.989		9.343	
10.22	4.166			

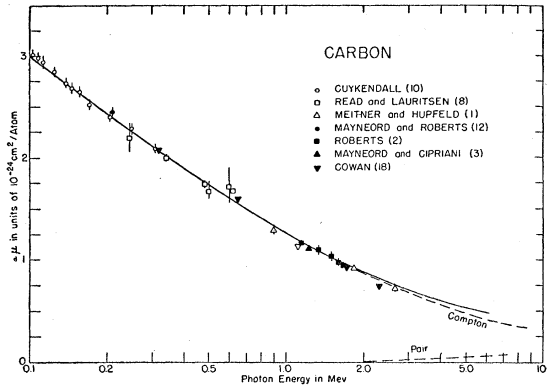

FIG. 28.

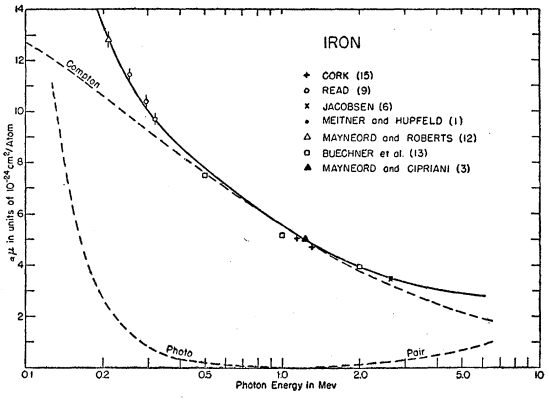

FIG. 31.

one energy. In this case the absorption coefficient can be calculated directly from the measured transmission by use of Eq. (2). However, many sources emit photons of more than one energy, and in this case the measured

where η_i is the fraction of photons of the ith energy emitted by the source, ϵ_i is the relative efficiency of the detector for photons of this energy, and μ_i is the absorption coefficient for photons of this energy.

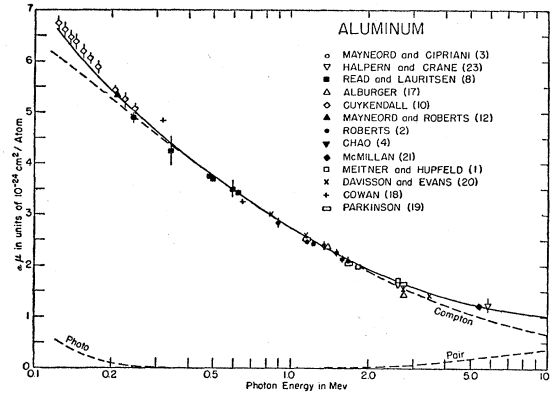

FIG. 29.

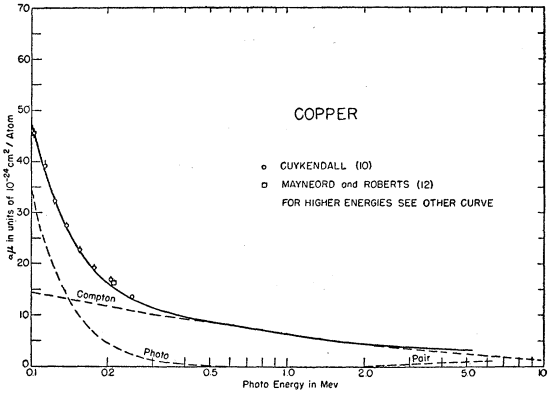

FIG. 32.

transmission must be compared with the expected transmission. The transmission expected is obtained from the equation

$$T=\sum_i \epsilon_i\eta_i e^{-\mu_i x}/\sum_i \epsilon_i\eta_i, \qquad (62)$$

If a source emits more than one energy and is also very long, the different energies will be absorbed by different amounts within the source itself, so that η_i of Eq. (62) will depend on the length of the source. Correc-

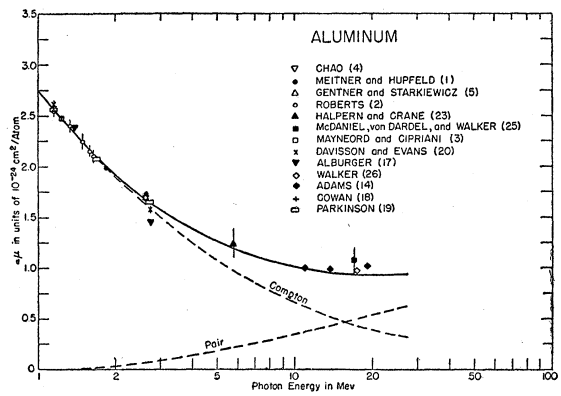

FIG. 30.

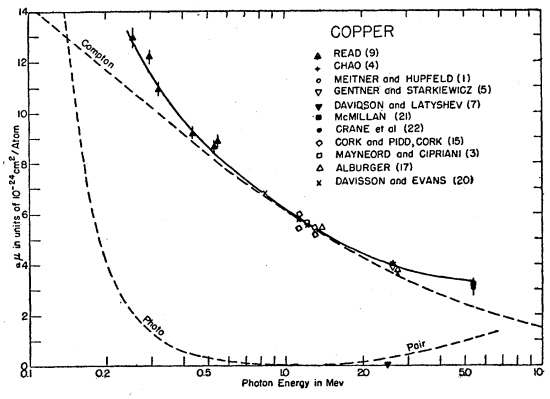

FIG. 33.

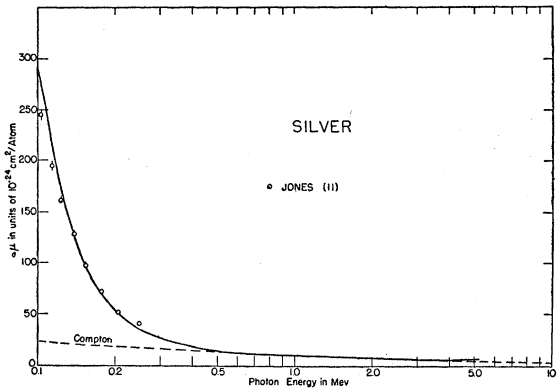

FIG. 34.

tion for this can be made with the following formula, which gives the ratio of the number of photons of any one energy emitted from the end of the source to those which would be emitted if there were no self-absorption:

$$(1-e^{-\mu l})/\mu l. \tag{63}$$

Here l is the length of the source.

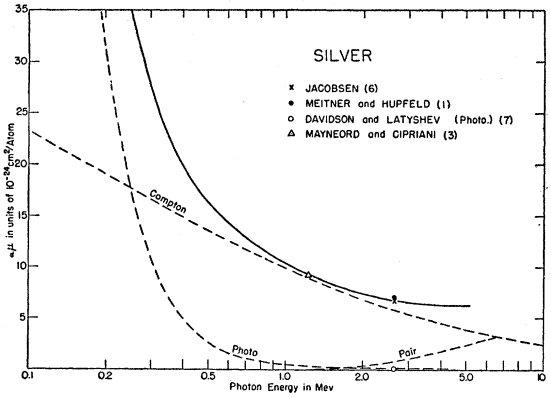

FIG. 35.

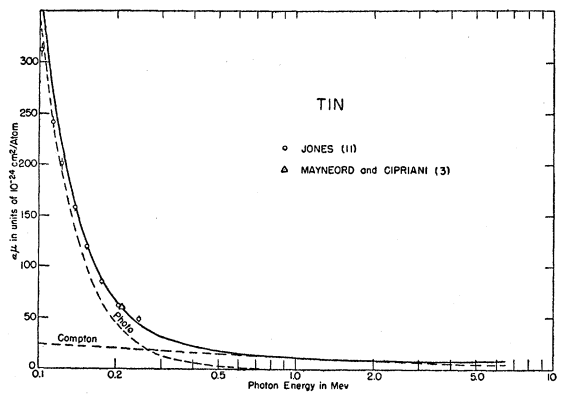

FIG. 36.

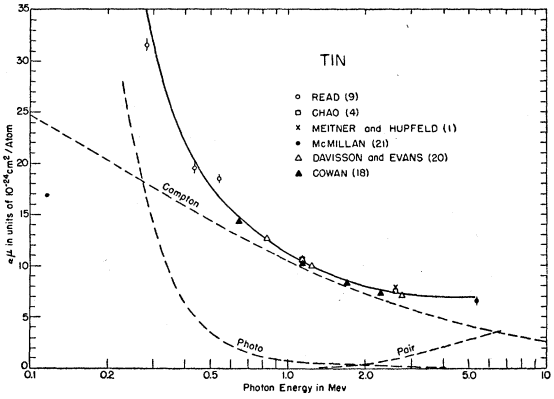

FIG. 37.

2. *Absorbers*

The main requirement for an absorber is that its composition and its thickness be known. For measuring the absorption coefficients of elements, samples which are as pure as possible should be used. If compounds or mixtures are used, the intensity of radiation absorbed in a thickness dx is

$$dI=I[(\mu_1/\rho_1)a_1+(\mu_2/\rho_2)a_2+(\mu_3/\rho_3)a_3+\cdots]Mdx, \tag{64}$$

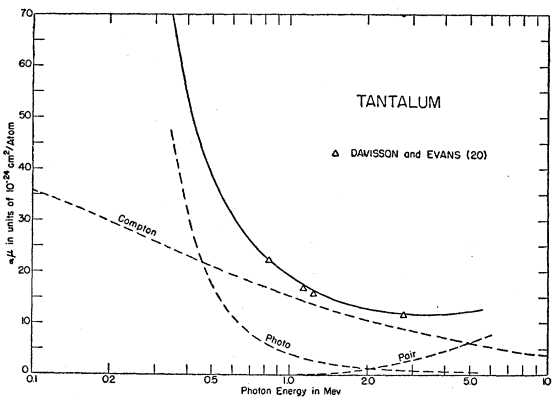

FIG. 38.

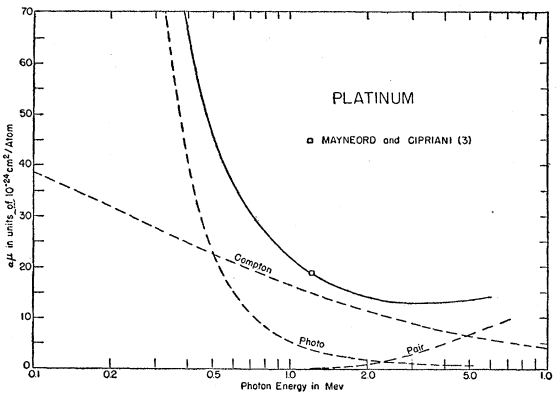

FIG. 39.

where a_1, a_2, $\cdots$ are the fractional amounts by weight of the various elements present in the absorber, and M is the total density. Measurements on the compound yield the effective mass absorption coefficient $[(\mu_1/\rho_1)a_1 + (\mu_2/\rho_2)a_2 + \cdots]$. To find the individual values of μ/ρ, it is necessary either to measure mixtures of the same elements, that have different fractional amounts by weight, or to obtain all but one of the coefficients by other methods.

3. Detectors

The four general types of detectors which can be used are cloud chambers, ionization chambers, Geiger-Müller counters, and crystal counters. In all of them it is not the photons directly but the secondary electrons or light produced by the photons which are detected and measured.

In a cloud chamber it is the individual electron tracks which are studied. Since the energies of the electrons produced by Compton effect, photoelectric effect, and pair production are different, the secondaries produced by the different effects, and their angular distribution, can be studied separately. Also, since the individual electron energies can be measured, those electrons produced by the lower energy scattered radiation can be eliminated from the measurements. Moreover, if the source emits photons of widely differing energies, the electrons produced by the different energies can be studied separately. The cloud chamber, however, has serious disadvantages in that the adjustments for proper operation are critical; the measurements on the individual tracks are often tedious; and the number of measurements possible in a given time is comparatively few, so that the statistical error of the results may be larger than with other detectors.

In an ionization chamber the secondary electrons ionize the gas of the chamber, and the rate of collection of the charge on the chamber electrodes is the quantity measured. The number of ions produced, and thus their rate of collection, depends on the chamber material, the nature and amount of the gas in the chamber, and the energy necessary to produce an ion pair. These have been studied by L. H. Gray and others[30] and the amount of ionization produced, as a function of the amount of photon energy absorbed, can be determined.

In a Geiger-Müller counter the secondary electrons serve only to trigger a gas discharge. The counting rate, therefore, depends only on the number of electrons entering the sensitive volume of the counter and not on their energy. Since the amount of gas in the counter is usually small, comparatively few electrons are produced in the gas volume so the counting rate is directly proportional to the number of electrons entering the gas from the counter walls. This number depends on the photon energy only through the absorption coefficients of the counter wall and the range of the electrons in the wall material, so the efficiency of a counter as a function of photon energy is somewhat less difficult to determine than the efficiency of an ionization chamber. Counter efficiencies have been studied both theoretically[31] and experimentally.[32] Counters made of materials of high atomic number have the greatest efficiency, but those made of copper or elements in the same range of atomic number have efficiencies which are very nearly proportional to the photon energy, at least in the energy range from 0.1 Mev to 6 Mev which we are considering.

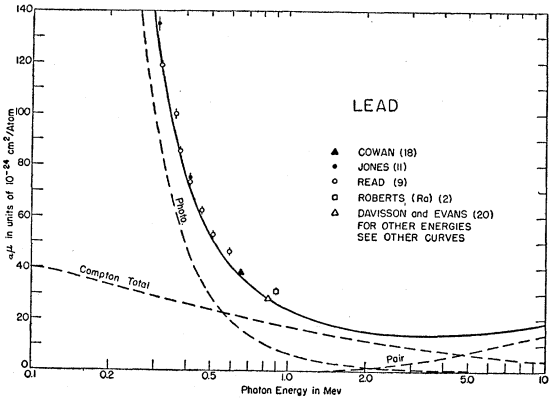

FIG. 41.

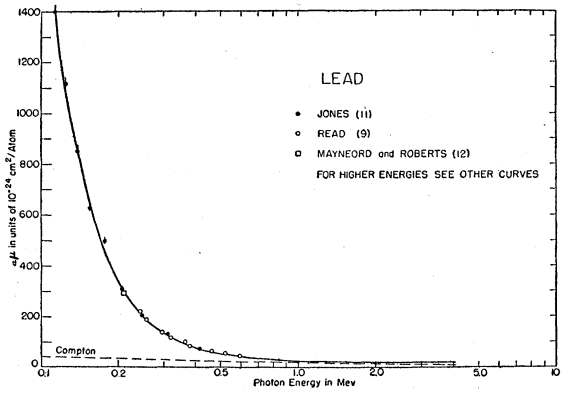

FIG. 40.

[30] L. H. Gray, Proc. Roy. Soc. (London) **156A**, 578 (1936); J. A. Chalmers, Phil. Mag. **6**, 745 (1928); L. Bastings, J. Sci. Instr. **5**, 113 (1928); E. C. Stoner, Phil. Mag. **7**, 841 (1929); E. J. Workman, Phys. Rev. **43**, 859 (1933); J. R. Clarkson, Phil. Mag. **31**, 437 (1941); B. B. Rossi and H. H. Staub, National Nuclear Energy Series, Manhattan Project Technical Section, Division V, Vol. 2 (McGraw-Hill Book Company, Inc., New York, 1949).

[31] G. von Droste, Z. Physik **100**, 529 (1936); H. Yukawa and S. Sakata, Tokyo Inst. Phys. Chem. Research Sci. Papers **31**, No. 686, 187 (1937).

[32] N. Marty, J. phys. et radium **8**, 29 (1947); J. V. Dunworth, Rev. Sci. Instr. **11**, 167 (1940); G. J. Sizoo and H. Willemsen, Physica **5**, 105 (1938); F. Norling, Phys. Rev. **58**, 277 (1940), and Arkiv. Mat. Astrom. Fysik **27B**, No. 27 (1940); Roberts, Downing, and Deutsch, Phys. Rev. **60**, 544 (1941); Roberts, Elliott, Downing, Peacock, and Deutsch, Phys. Rev. **64**, 268 (1943); W. Peacock, Ph.D. thesis, M.I.T. 1944 and Phys. Rev. **66**, 160 (1944); H. Maier-Leibnitz, Z. Naturforsch. **1**, 243 (1946); Bradt, Gugelot, Huber, Medicus, Preiswerk, and Scherrer, Helv. Phys. Acta **19**, 77 (1946).

When such counters are used, the detector efficiency, ϵ_i of Eq. (62), can be placed equal to the photon energy, and the comparison of experimental results with theoretical predictions is comparatively simple.

There are two types of crystal counters, conduction[33] and scintillation.[34] The conduction-type counter measures the current resulting from the ionization produced in the crystal by the radiation, while the scintillation counter detects the light emitted by the phosphor after the radiation has excited and ionized the molecules of the crystal. The two types have certain advantages in common: (1) Because of the greater absorption of γ-rays in a solid than in a gas, their efficiency for counting γ-rays is much greater than the gaseous counter and may be the order of 10 to 20 percent, depending on the kind of crystal and its size. (2) The counter dimensions may be much smaller than the gaseous counters, so they can be used conveniently in narrow beam geometry. (3) Both have short resolving times (the order of 10^{-8} sec for some crystals). (4) There is no initial delay of the pulse. (5) The pulse height is linearly proportional to the energy of the ionizing radiation (i.e., the β-rays or the secondary electrons). (6) They require no vacuum-tight envelope, so offer no window absorption problem when detecting low energies. In addition the scintillation counter has a very long lifetime and comparatively constant working characteristics. However, at low intensities the dark current noise of the photomultiplier used with the scintillation counter may be troublesome, and if a large crystal is used or the radiation to be detected is at some distance from the electronic equipment, the collection or the "piping" of the light may be a problem. The conduction-type counter has the advantage that a large crystal can be used without any light collection problem. However, the conduction counter at present has the disadvantages that (1) because of polarization effects the pulse size may vary during an experiment and (2) the only suitable large crystals known at present must be carefully annealled, held at low temperatures, and kept under a vacuum, though there are a few small crystals, such as diamond, suitable for room temperature work.

4. Geometry

The geometry of the apparatus for studying absorption coefficients is determined mainly from considerations of scattered radiation, since most of the difficulties encountered arise from secondary radiation which may reach the detector. Such secondary radiation, which may be Compton scattered radiation, annihilation radiation, or bremsstrahlung from secondary electrons, may have been scattered into the detector by nearby objects, or it may have been produced in the absorber itself at such an angle as to be able to reach the detector.

[33] R. Hofstadter, Nucleonics 4, 2 (1949); 4, 29 (1949).
[34] W. H. Jordan and P. R. Bell, Nucleonics 5, 30 (1949); J. W. Coltman, Proc. Inst. Radio Engrs. 37, 671 (1949).

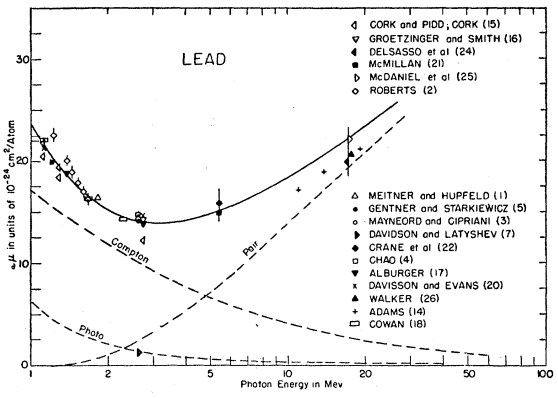

FIG. 42.

FIGS. 28 to 42. Absorption coefficients *vs* energy for some elements. Smooth curves are theoretical values. Points are experimental values of different workers. Numbers in parentheses after names refer to the following references:

[1] L. Meitner and H. H. Hupfeld, Z. Physik **67**, 147 (1931).
[2] J. E. Roberts, Proc. Roy. Soc. (London) **183A**, 338 (1945).
[3] W. V. Mayneord and A. J. Cipriani, Can. J. Research **25A**, 303 (1947).
[4] C. Y. Chao, Proc. Natl. Acad. Sci. **16**, 431 (1930).
[5] W. Gentner and J. Starkiewicz, J. phys. et radium **6**, 340 (1935).
[6] J. C. Jacobsen, Z. Physik **103**, 747 (1936).
[7] Z. S. Davidson and G. D. Latyshev, J. Phys. (U.S.S.R.) **6**, 15 (1942).
[8] J. Read and C. C. Lauritsen, Phys. Rev. **45**, 433 (1934).
[9] J. Read, Proc. Roy. Soc. (London) **152A**, 402 (1935).
[10] T. R. Cuykendall, Phys. Rev. **50**, 105 (1936).
[11] M. T. Jones, Phys. Rev. **50**, 110 (1936).
[12] W. V. Mayneord and J. E. Roberts, Nature **136**, 793 (1935).
[13] Buechner, Van de Graaff, Feshbach, Burrill, Sperduto, and McIntosh, Am. Soc. Testing Materials, Bull. No. 155, December, 1948.
[14] G. D. Adams, Phys. Rev. **74**, 1707 (1948).
[15] J. M. Cork and R. W. Pidd, Phys. Rev. **66**, 227 (1944); and J. M. Cork, Phys. Rev. **67**, 53 (1945).
[16] G. Groetzinger and L. Smith, Phys. Rev. **67**, 53 (1945).
[17] D. E. Alburger, Phys. Rev. **73**, 344 (1948).
[18] C. L. Cowan, Phys. Rev. **74**, 1841 (1948).
[19] W. C. Parkinson, Phys. Rev. **76**, 1348 (1949).
[20] C. M. Davisson and R. D. Evans, Phys. Rev. **81**, 404 (1951).
[21] E. M. McMillan, Phys. Rev. **46**, 868 (1934).
[22] Crane, Delsasso, Fowler, and Lauritsen, Phys. Rev. **46**, 531 (1934).
[23] J. Halpern and H. R. Crane, Phys. Rev. **55**, 258 (1939).
[24] Delsasso, Fowler, and Lauritsen, Phys. Rev. **51**, 391 (1937).
[25] McDaniel, von Dardel, and Walker, Phys. Rev. **72**, 985 (1947).
[26] R. L. Walker, Phys. Rev. **76**, 527 (1949).

The geometry must either be such that the amount of secondary radiation reaching the detector is negligible or such that corrections can be made for it.

There are two methods of preventing radiation from nearby objects from reaching the detector. One is to keep both the source and the detector at large distances from surrounding objects so that, because of distance and angle considerations, the amount of radiation which can be scattered is small. The other is to use a large amount of lead or other absorbing material around both the source and the detector so that the amount of radiation available for scattering by room objects is small and at the same time so that what little is scat-

tered will be absorbed before reaching the detector. If the lead is available, the latter method is a bit more satisfactory, as it permits experiments to be carried out in a small laboratory room. Moreover, if the first method is used, it is possible that scattering from the air may affect the results somewhat.[35]

The secondary radiation produced in the absorber itself is more difficult to eliminate from the measurements. In estimating the amount of such scattered or secondary radiation which can reach the detector, both the geometry of the apparatus and the characteristics of the secondary radiation must be considered. This has been done for Compton scattering by Tarrant[6] who makes an analysis of singly-scattered radiation reaching the detector.

Tarrant studies the geometry shown in Fig. 43 and assumes the source to emit photons of a single energy. Considering the radiation falling on the annular ring of volume $2\pi ydydx$ and the number scattered by it to the detector at the scattering angle θ, Tarrant obtains the following equation for the number of photons scattered into the detector per unit time by this volume element:

$$dS=[B_0(\cos^2\varphi_1/l_1^2)2\pi ydye^{-\mu_1 x\sec\varphi_1}][k(\theta)N_e dx]\times[e^{-\mu_2(x_0-x)\sec\varphi_2}][D/(l_2^2\sec^2\varphi_2)]. \quad (65)$$

Here B_0 is the number of photons per unit solid angle

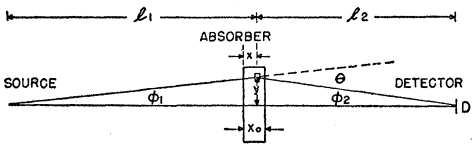

FIG. 43. Diagram for analysis of scattering from the absorber.

emitted by the source per second; μ_1 is the absorption coefficient of the primary radiation; μ_2 is the absorption coefficient of the radiation scattered at the angle θ; N_e is the number of electrons per unit volume in the absorber; D is the area of the detector; and $k(\theta)$ is the cross section in cm^2/electron for the number of photons scattered into unit solid angle in the direction θ (see Eq. (16)). The first bracket in the equation represents the number of photons incident on the annular ring per second; the second bracket is the fraction of the photons scattered per unit solid angle in the direction θ; the third represents the loss in the number of scattered photons due to absorption in the absorber; and the last bracket is essentially the solid angle subtended by the detector at any point of the scattering volume. By integrating with respect to x, putting

$$\cos^2\varphi_1\cos^2\varphi_2 ydy/l_1^2l_2^2=X\sin\theta d\theta/(l_1+l_2)^2$$

with

$$X=[1+y^2(l_1-l_2)^2/(y^2+l_1l_2)^2]^{\frac{3}{2}} \quad (66)$$

and putting $\delta=\mu_2\sec\varphi_2-\mu_1\sec\varphi_1$, it can be shown that the total amount of singly scattered radiation detected by the counter or the ionization chamber is

$$S=[B_0D\epsilon_0/(l_1+l_2)^2]N_e x_0 e^{-\mu_1 x_0}\times\int_0^{\theta_0} X(\epsilon_\theta/\epsilon_0)e^{-\mu_1 x_0(\sec\varphi_1-1)}\times[(e^{-\delta x_0}-1)/\delta x_0]k(\theta)2\pi\sin\theta d\theta, \quad (67)$$

where ϵ_θ is the detector efficiency for the radiation scattered at the angle θ, ϵ_0 is the detector efficiency for the primary radiation, and θ_0 is the maximum angle of scattering for radiation entering the center of the detector. In most practical cases where small sources and absorbers of small diameter are used, the angles involved are small and the energy of the scattered photons differs little from the primary energy, so that $e^{-\mu_1 x_0(\sec\varphi_1-1)}$, $(e^{-\delta x_0}-1)/\delta x_0$, and $\epsilon_\theta/\epsilon_0$ are close to unity for all values of θ intercepted by the detector. Also, if the absorber is not close to either the source or the detector, X is close to unity. Therefore the number of scattered photons measured by the detector is

$$S=[B_0D\epsilon_0/(l_1+l_2)^2]N_e x_0 e^{-\mu_1 x_0}\int_0^{\theta_0} 2\pi k(\theta)\sin\theta d\theta$$
$$=[B_0D\epsilon_0/(l_1+l_2)^2]N_e x_0 e^{-\mu_1 x_0}{}_e\sigma^{\theta_0}, \quad (68)$$

where ${}_e\sigma^{\theta_0}$ is the cross section for the number of photons scattered between 0 and θ_0 and is given by Eq. (25). Since the number of primary photons measured by the detector is

$$B=[B_0D\epsilon_0/(l_1+l_2)^2]e^{-\mu_1 x_0}, \quad (69)$$

the ratio of the number of scattered to the number of transmitted photons is

$$S/B=N_e x_0{}_e\sigma^{\theta_0}. \quad (70)$$

If the efficiency of the detector is proportional to the energies of the photons to be measured as in the case of a copper cathode counter, account may be taken of the fact that $\epsilon_\theta/\epsilon_0$ is not unity. In this case $\epsilon_\theta/\epsilon_0=\nu_\theta/\nu_0$ and, still assuming the other factors to be close to unity, Eq. (68) becomes

$$S=[B_0D\epsilon_0/(l_1+l_2)^2]N_e x_0 e^{-\mu_1 x_0}\times\int_0^{\theta_0} 2\pi(\nu_\theta/\nu_0)k(\theta)\sin\theta d\theta. \quad (71)$$

But $(\nu_\theta/\nu_0)k(\theta)$ is the cross section per unit solid angle for the photon energy scattered in the direction θ and is given by Eq. (18). Therefore the ratio of the number of scattered to the number of transmitted photons, as measured by the detector, is

$$S/B=N_e x_0{}_e\sigma_s{}^{\theta_0}, \quad (72)$$

where ${}_e\sigma_s{}^{\theta_0}$ is the cross section for the energy of the photons scattered between 0 and θ_0 and is given by

[35] C. L. Cowan, Phys. Rev. 74, 1841 (1948).

Eq. (26). Since the angles involved in most scattering experiments are small, the approximations for ${}_e\sigma^{\theta_0}$ and ${}_e\sigma_s{}^{\theta_0}$, as given in Eq. (31), can be used, i.e.,

$$ {}_e\sigma^{\theta_0} = {}_e\sigma_s{}^{\theta_0} = \pi r_0{}^2\theta_0{}^2. $$

This shows that for small angles the amount of scattered radiation reaching the detectors is independent of the photon energy and is proportional to the solid angle of the scattering cone being considered.

We can now estimate the maximum allowable angle, θ_0, for any arbitrarily chosen value of S/B. This is done in Table XV for 2.76-Mev γ-rays and a transmission of 0.1 percent. With available source strengths it is unlikely that a transmission of 0.001 could be measured to better than 1 percent, so with a scattering angle of 1.5° to 2° no correction would need to be made for single scattering.

For thick absorbers some of the singly-scattered photons, which in Eq. (65) were considered as lost (third bracket of the equation), will be scattered and rescattered. Some may finally reach the detector and cause the ratio of scattered to transmitted to be greater than the values given by Eqs. (70) or (72). An accurate analysis of this double and multiple scattering, using the Klein-Nishina theory of Compton scattering is difficult. Early attempts were made by Bopp[36] and Tandberg.[37] Recently, due to interest in shielding and dosage problems much more work has been done along this line.[38] One would expect, however, that in the energy range being considered, the multiply-scattered radiation reaching the detector would be much less than the singly-scattered radiation which reaches it, so that if the scattering angles are kept small, it could be neglected.

Considerations of the secondary radiation reaching the detector due to the annihilation radiation from positrons produced in pair production or to bremsstrahlung produced by secondary electrons follows the same line of reasoning as that which led to Eq. (65) with the corresponding pair production, photoelectric, and bremsstrahlung coefficients replacing $k(\theta)$. It is to be expected that the secondary radiation reaching the detector resulting from these effects is much less than that resulting from single Compton scattering. In the case of annihilation radiation the cross section for pair production is, in the energy region we are considering, less than that for the Compton effect, and in addition, the annihilation radiation is emitted isotropically. In the case of bremsstrahlung the bremsstrahlung cross sections, combined with those for the production of the secondary electrons, is certainly much less than the Compton cross sections.

It is to be noted in considering scattering from the absorber that the maximum scattering angle for scattered rays reaching the detector increases with absorber diameter and depends also on the position of the absorber between the source and the detector. For minimum scattering, especially with no added collimation after the absorber, the absorber diameter should be no larger than is necessary for the absorber to intercept the cone of radiation incident on the detector and should be located half-way between the source and the detector.

Another geometrical factor which must be considered is the divergence of the beam, with the accompanying difference in path length through the absorber for different parts of the beam. Analytical expressions for taking account of this divergence have been derived by Soddy and Russell,[39] King,[40] and Tandberg.[37] However, it is not until the divergence of the beam is very large that this effect must be taken into account.

TABLE XV. Cross sections and maximum angle of scattering for a transmission of 0.001 with 2.76 Mev γ-rays, for various ratios, S/B, of scattered to transmitted photons.

Element	Electrons per cc	Absorber thickness for T =0.001 (cm)	$N_e x_0$ (electrons per cm²)	Cross section in cm²/electron if S/B is 0.001	0.01	0.1
Al	7.86×10^{23}	69.7	5.48×10^{25}	1.82×10^{-29}	1.82×10^{-28}	1.82×10^{-27}
Cu	2.46×10^{24}	21.2	5.20×10^{24}	1.92×10^{-29}	1.92×10^{-28}	1.92×10^{-27}
Sn	1.85×10^{24}	25.5	4.72×10^{25}	2.12×10^{-29}	2.12×10^{-28}	2.12×10^{-27}
Pb	2.71×10^{24}	14.8	4.00×10^{25}	2.50×10^{-29}	2.50×10^{-28}	2.50×10^{-27}
Maximum scattering angle, θ_0				0.5°	1.6°	5°–6°

Different geometries have been used by different workers. One which we have used and found extremely satisfactory is shown diagrammatically in Fig. 44. The source-to-detector distance was about 125 cm. Thus, with a detector 2 cm in diameter the beam of γ-rays from the source to the detector formed a cone whose half-angle was 0.5°. The maximum angle θ_0 at which a γ-ray could be scattered from the edge of the absorber next to the lead shield C and still reach the detector was 1.3° for a γ-ray from the center of the source scattered to the center of the detector (2.6° from edge of source to edge of detector). For this geometry, therefore, no correction for scattered radiation needed to be made. The amount of lead around the source and the detector was such that the minimum thickness through which a γ-ray which might be scattered from room objects had to pass was 4 cm at the source and 11 cm at the counter. This much lead would reduce the intensity of 2.76-Mev γ-rays

[36] F. Bopp, Ann. Physik **30**, 35 (1937).
[37] J. Tandberg, Arkiv. Mat. Astron. Fysik **27B**, No. 3 (1940).
[38] Hirschfelder, Magee, and Hull, Phys. Rev. **73**, 852 (1948); J. O. Hirschfelder and E. N. Adams, II, Phys. Rev. **73**, 863 (1948); W. R. Faust and M. H. Johnson, Phys. Rev. **75**, 467 (1949); U. Fano and P. R. Karr, Phys. Rev. **75**, 1303 (1949); Bethe, Fano, and Karr, Phys. Rev. **76**, 538 (1949); U. Fano, Phys. Rev. **76**, 739 (1949); P. R. Karr and J. C. Lamkin, Phys. Rev. **76**, 1843 (1949); Fano, Hurwitz, and Spencer, Phys. Rev. **77**, 425 (1950); L. L. Foldy, Phys. Rev. **81**, 395 (1951); L. L. Foldy and R. K. Osborn, Phys. Rev. **81**, 400 (1951); G. H. Peebles and M. S. Plesset, Phys. Rev. **81**, 430 (1951); L. V. Spencer and U. Fano, Phys. Rev. **81**, 464 (1951); Cave, Corner, and Liston, Proc. Roy. Soc. (London) **204A**, 223 (1950); J. Corner, and R. H. A. Liston, Proc. Roy. Soc. (London) **204A**, 323 (1950); Corner, Day, and Weir, Proc. Roy. Soc. (London) **204A**, 329 (1950).
[39] Soddy, Soddy, and Russell, Phil. Mag. **19**, 725 (1910).
[40] L. V. King, Phil. Mag. **23**, 242 (1912).

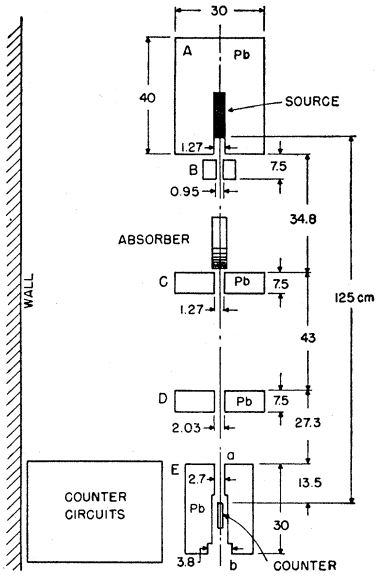

FIG. 44. A schematic plan view of apparatus and collimating system for the measurement of total absorption coefficients, which has been very satisfactory. All dimensions are shown in cm.

to 0.1 percent. Our tests with Co^{60} γ-rays and a copper absorber showed that without the lead shield C after the absorbers the scattered radiation became appreciable for transmissions less than 0.005. With the lead shield C, however, the semilog plot of the measured transmission was a straight line, having the expected slope, to transmissions as low as 0.0002.

Experimental Results

On the curves of Figs. 28 to 42 are included the experimental values of various workers. In Table XVI they are listed according to the type of source which was used.

Radium with its decay products is a very poor source to use in finding the variation of absorption coefficients with γ-ray energy because its γ-ray spectrum is very complex.[41–45] However, some excellent work has been done with radium, e.g., that of Kohlrausch.[46] Moreover, because of its availability it has been studied by many workers and is sometimes convenient to use for checking apparatus and for comparison of results from different laboratories. For this reason we have calculated the transmission in lead to be expected theoretically for different conditions. They are given in Fig. 45. The dashed lines show the results expected if the detector is equally sensitive to all energies, while the solid lines show those expected if the detector sensitivity is proportional to the energy. Curves A were calculated with the spectral and intensity distribution given by Ellis and Aston.[41,47] Curves B were calculated with the energy and intensity values given by Latyshev[45] but were supplemented with the low energy values given by Ellis and Aston. The relative intensities of the Russian and English workers were compared by referring them both to the intensity of the 2.198-Mev γ-ray, which was taken as unity. Curve C shows the transmission expected if all the radiation scattered in the absorber reaches the

TABLE XVI. Previous studies of absorption coefficients.

Sources and workers (Remarks)	References
Radium as source	
K. W. F. Kohlrausch (Analysis by G. J. Sizoo and H. Willemsen (Physica **5**, 100 (1938)) shows good agreement with theory.)	Sitzber. Akad. Wiss. Wien **126IIa**, 441, 683, 887 (1917); Handbuch Exp. Phys. **15**, 78 (1928).
J. H. Gray and H. M. Cave	Trans. Roy. Soc. Can. **21**, 163 (1927).
L. Meitner and H. H. Hupfeld	Z. Physik **67**, 147 (1931).
J. S. Rogers	Proc. Phys. Soc. (London) **44**, 349 (1932).
H. Ketelaar, A. Piccard, and E. Stahel	J. phys. et radium **5**, 385 (1934).
I. Zlotowski	J. phys. et radium **6**, 242 (1935).
J. E. Roberts	Proc. Roy. Soc. (London) **183A**, 338 (1945).
W. V. Mayneord and A. J. Cipriani	Can. J. Research **25A**, 303 (1947).
ThC″ as source	
C. Y. Chao	Proc. Natl. Acad. Sci. **16**, 431 (1930).
L. Meitner and H. H. Hupfeld	Z. Physik **67**, 147 (1931).
G. T. P. Tarrant	Proc. Roy. Soc. (London) **135A**, 223 (1932).
W. Gentner and J. Starkiewicz	J. phys. et radium **6**, 340 (1935).
J. C. Jacobsen (Good review of above articles by W. Gentner)	Z. Physik **103**, 747 (1936). Physik. Z. **38**, 836 (1937).
K. Zuber (Pair production only)	Helv. Phys. Acta **15**, 38 (1942).
Z. S. Davidson and G. D. Latyshev (Photoelectric effect only)	J. Phys. (U.S.S.R.) **6**, 15 (1942).
X-rays as source	
J. Read and C. C. Lauritsen	Phys. Rev. **45**, 433 (1934).
J. Read	Proc. Roy. Soc. (London) **152A**, 402 (1935).
T. R. Cuykendall	Phys. Rev. **50**, 105 (1936).
M. T. Jones	Phys. Rev. **50**, 110 (1936).
W. V. Mayneord and J. E. Roberts	Nature **136**, 793 (1935).
W. W. Buechner, R. J. Van de Graaff, H. Feshbach, E. A. Burrill, Jr., A. Sperduto, and R. McIntosh	Am. Soc. Testing Materials, Bull. No. 155, Dec. 1948.
G. D. Adams	Phys. Rev. **74**, 1707 (1948).
J. L. Lawson	Phys. Rev. **75**, 433 (1949).
γ-rays from artificially radioactive substances as source	
J. M. Cork and R. W. Pidd	Phys. Rev. **66**, 227 (1944).
J. M. Cork	Phys. Rev. **67**, 53 (1945).
G. Groetzinger and L. Smith	Phys. Rev. **67**, 53 (1945).
W. V. Mayneord and A. J. Cipriani	Can. J. Research **25A**, 303 (1947).
D. E. Alburger	Phys. Rev. **73**, 344 (1948).
C. L. Cowan	Phys. Rev. **74**, 1841 (1948).
W. C. Parkinson	Phys. Rev. **76**, 1348 (1949).
C. M. Davisson and R. D. Evans	Phys. Rev. **81**, 404 (1951).
γ-rays from nuclear reactions as source	
E. M. McMillan ($F+p$)	Phys. Rev. **46**, 868 (1934).
H. R. Crane, L. A. Delsasso, W. A. Fowler, and C. C. Lauritsen ($Li+p$ and $F+p$)	Phys. Rev. **46**, 531 (1934).
J. Halpern and H. R. Crane ($F+p$)	Phys. Rev. **55**, 258 (1939).
L. A. Delsasso, W. A. Fowler, and C. C. Lauritsen ($Li+p$)	Phys. Rev. **51**, 391 (1937).
B. D. McDaniel, G. von Dardel, and R. L. Walker ($Li+p$)	Phys. Rev. **72**, 985 (1947).
R. L. Walker ($Li+p$)	Phys. Rev. **76**, (1949).

[41] C. D. Ellis and G. H. Aston, Proc. Roy. Soc. (London) **129A**, 180 (1930).
[42] D. Skobeltzyn, Z. Physik **58**, 595 (1929).
[43] E. Stahel and W. Johner, J. phys. et radium **5**, 97 (1934).
[44] C. D. Ellis, Proc. Roy. Soc. (London) **143A**, 350 (1933).
[45] G. D. Latyshev, Revs. Modern Phys. **19**, 132 (1947).
[46] K. W. F. Kohlrausch, Sitzber. Akad. Wiss. Wien **126IIa**, 441, 683, 887 (1917); Handbuch Exp. Phys. **15**, 78 (1928).
[47] R. D. Evans, Nucleonics **1**, No. 2, 32 (1947).

detector, while curves A and B show that expected if none reaches the detector. If scattering is not negligible, the experimental results should lie between the two. The points shown on the curves are our experimental points[48] taken with the geometry shown in Fig. 44 and with a copper counter whose sensitivity was approximately proportional to the photon energy. Our results agree well with the curves for no scattering but are not accurate enough to show which of the two radium γ-ray spectra is the better.

Sources of RdTh and its decay products have a predominant γ-ray of 2.62 Mev from the decay of ThC''.[45,49–52] Although other γ-rays are also present, their intensity is comparatively small. Therefore with RdTh sources and sufficient initial absorber the absorption coefficients at 2.62 Mev can be studied. The total absorption coefficients measured with this source agree well with the theoretical values.[53] More recently, Davidson and Latyshev[13] have used the 2.62-Mev γ-ray of ThC'' to study the photoelectric absorption coefficient in lead at this energy, and Zuber[29] has used a RdTh source to study pair production coefficients in argon.

X-rays provide excellent sources for studying the absorption coefficients at low energies (<about 0.6 Mev). Although the radiation from an x-ray tube has a continuous distribution in energy, very nearly monochromatic radiation can be obtained by such means as balanced filtering[54] and reflection from crystals. In the energy region of about 0.1 to 0.5 Mev some careful studies of absorption coefficients have been made, which for the most part show good agreement with theory. Recent work with high energy beams is starting to extend x-ray absorption measurements to very high energies.[55,56]

Some artificially radioactive substances emit single energy γ-rays in the range from 0.4 Mev to 2.7 Mev, but until recently strong sources were not available. Comparatively little work has been done with these sources, therefore, and the results have not all shown agreement. With the geometry shown in Fig. 44 we have studied[48] the absorption in Al, Cu, Sn, Ta, and Pb of the γ-rays from I^{131}, Cu^{64}, Mn^{54}, Zn^{65}, Co^{60}, and Na^{24}. Our results show that in the energy range from 0.5 Mev to 2.8 Mev the experimental results agree with the theoretical values. In most cases this agreement was within 1.5 percent; although with Na^{24}, where the experimental errors were large, the agreement was only within 4 percent. Our results are in substantial agreement with those of Groetzinger and Smith,[57] Mayneord and Cipriani,[58] Cowan,[35] and Parkinson.[59] Our disagreement with some of the results of Alburger[60] and with the results of Cork and Pidd[61] and Cork[62] can be traced, we feel, to the poorer geometry of these workers and the possibility that the scattered radiation reaching their detectors was not negligible.

A few absorption measurements have been made with γ-rays of much higher energy by using those produced in the course of nuclear reactions. Absorption measurements with these sources are more difficult, so the

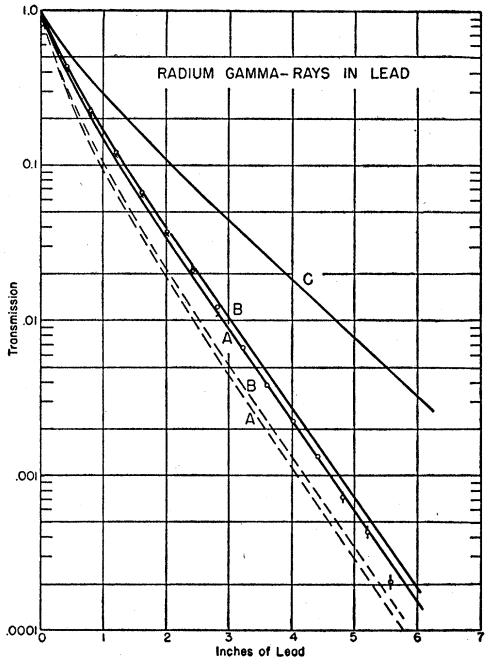

FIG. 45. Transmission through lead of γ-rays of radium in equilibrium with its decay products. Experimental points obtained with geometry shown in Fig. 44. *Crosses:* experimental points using 1.76-mg Ra salt in glass tube. *Solid circles:* experimental points using 27.7-mg Ra in a platinum cylinder of unknown wall thickness. The various theoretical transmission curves shown were calculated using the transmission through 0.5-mm Pt as unity. *Dashed curves:* assume detector sensitivity is independent of photon energy. *Solid curves:* assume detector sensitivity is linearly proportional to photon energy. *Curves A:* the number *vs* energy distribution in the γ-ray spectrum is taken from the data of C. D. Ellis and G. H. Aston (Proc. Roy. Soc. (London) **129A**, 180 (1930)) as compiled by R. D. Evans (Nucleonics **1**, No. 2, 32 (1947)). For each individual γ-ray component, the effective absorption coefficient is taken as $(\tau+\kappa+\sigma)$. *Curves B:* the γ-ray spectrum is a blend of Ellis and Aston for the low energy components up to 1.12 Mev and of G. D. Latyshev (Revs. Modern Phys. **19**, 132 (1947)) for the high energy components. Individual absorption coefficients $(\tau+\kappa+\sigma)$. *Curve C:* spectrum of Ellis and Aston: effective absorption coefficients taken as $(\tau+\kappa+\sigma-\sigma_s)$, i.e., as broad-beam with no scattered radiation excluded from the counter.

[48] C. M. Davisson and R. D. Evans, Phys. Rev. **81**, 404 (1951).
[49] C. D. Ellis, Proc. Phys. Soc. (London) **50**, 213 (1938).
[50] G. Stetter and W. Jentschke, Physik. Z. **40**, 104 (1939).
[51] J. L. Wolfson, Phys. Rev. **78**, 176 (1948).
[52] A. Hedgran, Phys. Rev. **82**, 128 (1951).
[53] W. Gentner, Physik. Z. **38**, 836 (1937).
[54] A. H. Compton and S. K. Allison, *X-rays in Theory and Experiment* (D. Van Nostrand Company, Inc., New York, 1935), p. 532.
[55] G. D. Adams, Phys. Rev. **74**, 1707 (1948).
[56] J. L. Lawson, Phys. Rev. **75**, 433 (1949).
[57] G. Groetzinger and L. Smith, Phys. Rev. **67**, 53 (1945).
[58] W. V. Mayneord and A. S. Cipriani, Can J. Research **25A**, 303 (1947).
[59] W. C. Parkinson, Phys. Rev. **76**, 1348 (1949).
[60] D. E. Alburger, Phys. Rev. **73**, 344 (1948).
[61] J. M. Cork and R. W. Pidd, Phys. Rev. **66**, 227 (1944).
[62] J. M. Cork, Phys. Rev. **67**, 53 (1945).

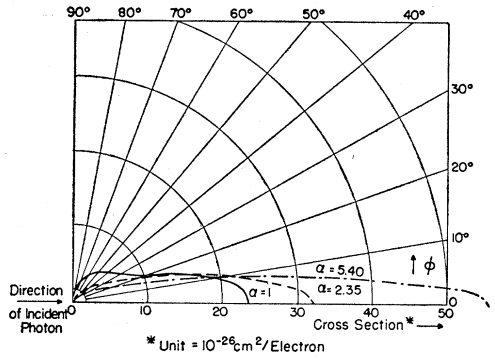

FIG. 46. Compton effect. Differential cross section per unit solid angle for the number of electrons scattered at the angle φ [Eq. (74)].

experimental errors are fairly large. However, most of the results show agreement with theory within the experimental errors.

From the comparison of experimental results with theory as given in Figs. 28 to 42, it can be concluded that in the energy range from 0.1 Mev to 6 Mev the present theories of Compton effect, photoelectric effect, and pair production give values of absorption coefficients which are in good agreement with the experimentally measured values.

Gamma-ray absorption coefficients have been calculated by Latter and Kahn[63] following the same procedure used in obtaining the values presented here with the exception that they used the Hulme-Jaeger values for low energy pair production and applied corrections for pair production in the field of the atomic electrons. In addition, an empirical formula, suggested by Jaeger, was used to relate the pair production cross sections for different elements at a given energy

$$\kappa(Z)=a\left(\frac{Z}{137}\right)^2+b\left(\frac{Z}{137}\right)^4.$$

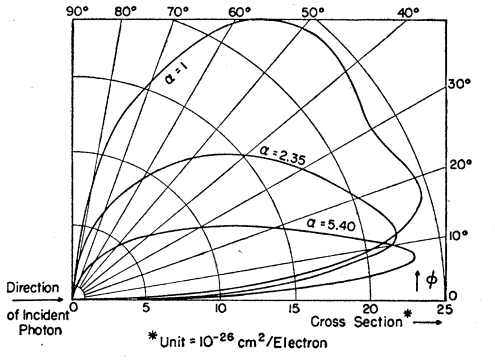

FIG. 47. Compton effect. Differential cross section per unit angle for the number of electrons scattered in the direction φ [Eq. (76)].

[63] R. Latter and H. Kahn, *Gamma-Ray Absorption Coefficients* (The Rand Corporation, 1949).

The constants are determined so that the first term is the Bethe-Heitler value and so that $K(Z=82)$ corresponds to the Hulme-Jaeger value for lead.

Since Latter and Kahn do not give specific values for τ and K, only the total coefficients μ and the sum of $\tau+K$ can be compared with the values presented here.

The values of $\tau+K$ disagree by as much as 13 percent, but the total coefficients show general agreement. For the light elements the agreement in μ is very good except at low energies such as 0.1 Mev. For the heavy elements the maximum differences occur again at low energies but with a difference peak of about 2.5 percent near 2 Mev.

Part of the discrepancies between the two calculations is probably due to over-correction in the pair production coefficient due to the Jaeger empirical formula, but a large part must be due to the inaccuracy inherent in the interpolation of photoelectric coefficients from published curves.

Gamma-ray absorption coefficients have also been calculated by G. R. White and are given in a report[64] to be published soon. This report covers the energy

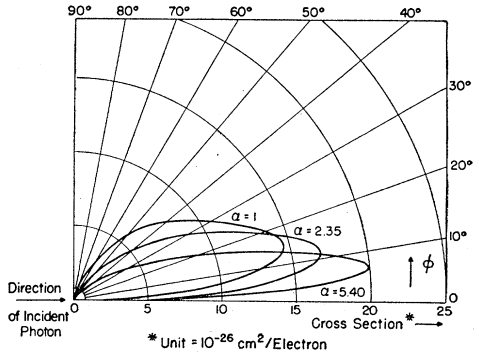

FIG. 48. Compton effect. Differential cross section per unit angle for the electron energy scattered in the direction φ [Eq. (77)].

range from 10 kev to 100 Mev. In the range we are considering these results are substantially the same as ours.

APPENDIX

Compton Electron Distribution||

Equations similar to those for the Compton photon distribution can be obtained for the Compton electron distribution. Since the probability that an electron will be scattered into the solid angle $d\Omega'$ situated in the direction φ is the same as the probability that a primary quantum will be scattered into the solid angle $d\Omega$ in the direction θ, θ and φ being related by Eq. (13), we have that

$$d_e\sigma=k(\theta)d\Omega=k(\varphi)d\Omega' \qquad (73)$$

[64] G. R. White, Natl. Bur. Standards Report No. 1003.

|| We are indebted to Dr. Gerald J. Hine, Special Research Fellow of the National Cancer Institute, Bethesda, Maryland, for initial calculations and for stimulating our interest in the equations for the Compton electron distribution.

or

$$(d_e\sigma/d\Omega')=k(\varphi)=k(\theta)(d\Omega/d\Omega'), \quad (74)$$

where $k(\theta)$ is given by Eq. (16). Analogous to Eqs. (18), (22), and (23) for photons we have for electrons

$$(d_e\sigma_a/d\Omega')=\kappa(\varphi)=(E_{el}/h\nu)k(\varphi) \quad (75)$$

$$(1/d\varphi)\int_{\varphi'=0}^{\varphi'=2\pi} d_e\sigma(\varphi)=2\pi\sin\varphi k(\varphi) \quad (76)$$

$$(1/d\varphi)\int_{\varphi'=0}^{\varphi'=2\pi} d_e\sigma_a(\varphi)=2\pi\sin\varphi\kappa(\varphi). \quad (77)$$

It can be shown that

$$d\Omega/d\Omega'$$
$$=-[4(1+\alpha)^2\cos\varphi]/[(1+\alpha)^2-\alpha(2+\alpha)\cos^2\varphi]^2 \quad (78)$$
$$=-[\sin\theta(1+\cos\theta)]/[(1+\alpha)\sin^3\varphi], \quad (79)$$

so that from values of $k(\theta)$ (see e.g., Table III) together with the energy and angular relationships of Eqs. (11), (12), and (13), these differential cross sections for electron scattering can be computed. Figures 46, 47, and 48 show some of these distributions when the primary photons are 0.511 Mev ($\alpha=1$), 1.2 Mev ($\alpha=2.35$), and 2.76 Mev ($\alpha=5.403$).

An additional quantity which is of interest is the differential cross section as a function of electron energy, which might be thought of as the number *vs* energy distribution of the electrons. Mathematically it would be

$$(d_e\sigma/dE_{el})=(d_e\sigma/d\varphi)(d\varphi/dE_{el}), \quad (80)$$

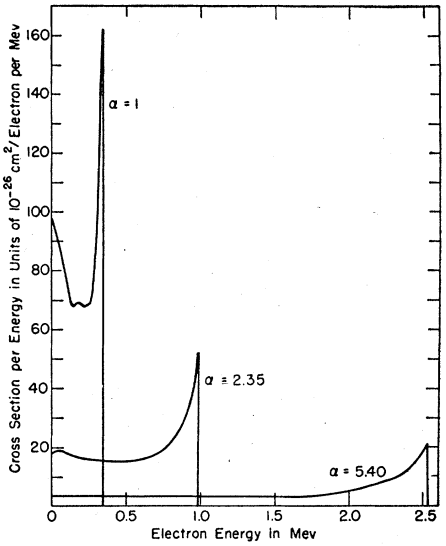

FIG. 49. Compton effect. Differential cross section per unit energy for the number of electrons scattered with the energy E_{el} (or the number of photons scattered with the energy $h\nu'=h\nu-E_{el}$) [Eq. (81)].

where $d_e\sigma/d\varphi$ is Eq. (76). This can be shown to be

$$(d_e\sigma/dE_{el})=(2\pi/\alpha h\nu)k(\theta)\{[(1+\alpha)^2-\alpha^2\cos^2\varphi] \div[(1+\alpha)^2-\alpha(2+\alpha)\cos^2\varphi]\}^2. \quad (81)$$

It is plotted in Fig. 49 for the same three primary photon energies, $\alpha=1$ (0.511 Mev), $\alpha=2.35$ (1.2 Mev), and $\alpha=5.403$ (2.76 Mev).